

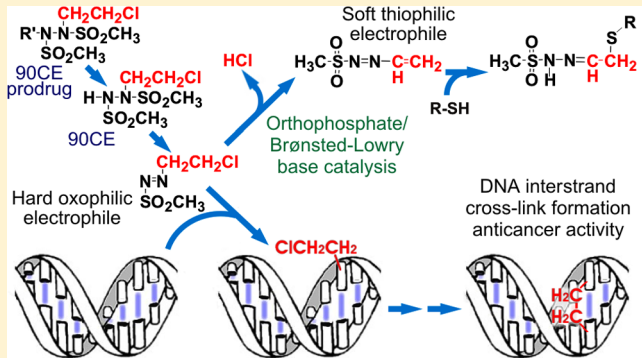
# Influence of Phosphate and Phosphoesters on the Decomposition Pathway of 1,2-Bis(methylsulfonyl)-1-(2-chloroethylhydrazine (90CE), the Active Anticancer Moiety Generated by Laromustine, KS119, and KS119W

Philip G. Penketh,\* Krishnamurthy Shyam, Rui Zhu, Raymond P. Baumann, Kimiko Ishiguro, and Alan C. Sartorelli

Department of Pharmacology and Yale Cancer Center, Yale University School of Medicine, 333 Cedar Street, New Haven, Connecticut 06520-8066, United States

## Supporting Information

**ABSTRACT:** Prodrugs of the short-lived chloroethylating agent 1,2-bis(methylsulfonyl)-1-(2-chloroethyl)hydrazine (90CE) and its methylating analogue 1,2-bis(methylsulfonyl)-1-(methyl)hydrazine (KS90) are potentially useful anticancer agents. This class of agents frequently yields higher ratios of therapeutically active oxophilic electrophiles responsible for DNA O<sup>6</sup>-guanine alkylations to other electrophiles with lower therapeutic relevance than the nitrosoureas. This results in improved selectivity toward tumors with diminished levels of O<sup>6</sup>-alkylguanine-DNA alkyltransferase (MGMT), the resistance protein responsible for O<sup>6</sup>-alkylguanine repair. The formation of O<sup>6</sup>-(2-chloroethyl)guanine, which leads to the formation of a DNA–DNA interstrand cross-link, accounts for the bulk of the anticancer activity of 90CE prodrugs. Herein, we describe a new decomposition pathway that is available to 90CE but not to its methylating counterpart. This pathway appears to be subject to general/acid base catalysis with phosphate (Pi), phosphomonoesters, and phosphodiesters, being particularly effective. This pathway does not yield a chloroethylating species and results in a major change in nucleophile preference since thiophilic rather than oxophilic electrophiles are produced. Thus, a Pi concentration dependent decrease in DNA–DNA interstrand cross-link formation was observed. Changes in 90CE decomposition products but not alkylation kinetics occurred in the presence of Pi since the prebranch point elimination of the N-1 methanesulfonate moiety remained the rate-limiting step. The Pi catalyzed route is expected to dominate at Pi and phosphoester concentrations totaling >25–35 mM. In view of the abundance of Pi and phosphoesters in cells, this pathway may have important effects on agent toxicity, tumor selectivity, and resistance to prodrugs of 90CE. Furthermore, it may be possible to design analogues that diminish this thiophile-generating pathway, which is likely superfluous at best and potentially detrimental to the targeting of hypoxic regions where Pi concentrations can be significantly elevated.



## INTRODUCTION

Laromustine (also called 101M, VNP40101M, cloretazine, and onargin), 1,2-bis(methylsulfonyl)-1-(2-chloroethyl)-2-[[(methylamino)carbonyl]hydrazine], KS119 (1,2-bis(methylsulfonyl)-1-(2-chloroethyl)-2-[[1-(4-nitrophenyl)ethoxy]carbonyl]hydrazine), and KS119W (1,2-bis(methylsulfonyl)-1-(2-chloroethyl)-2-[[1-(3-phospho-4-nitrophenyl)ethoxy]carbonyl]hydrazine) are relatively new anticancer alkylating agents.<sup>1–3</sup> These agents are all prodrugs of 90CE.<sup>1–3</sup> Laromustine, which has shown significant clinical activity in phase I and II clinical trials in AML,<sup>4</sup> generates 90CE upon base catalyzed decomposition; whereas, KS119 and KS119W generate 90CE when reductively activated, with the aim of adding selectivity toward hypoxic solid tumor regions.<sup>1–3</sup> The 90CE moiety has considerable potential in

tumor targeted prodrugs because it is an excellent leaving group, and the rapid spontaneous decomposition of 90CE ( $t_{1/2} \sim 30$  s), which can be prevented by the substitution of the N-2 hydrogen with a cleavable chemical trigger, results in the delivery of alkylation stress close to the site of activation.<sup>5,6</sup> The cytotoxic action of 90CE appears to result from the generation of chloroethylating intermediates that alkylate biomolecules, particularly the O-6 position of DNA guanine.<sup>7</sup> This latter alkylation accounts for the vast majority of its anticancer activity and leads to the eventual formation of a 1-(N<sup>3</sup>-cytosinyl),-2-(N<sup>1</sup>-guaninyl)ethane DNA–DNA interstrand cross-link (G-C ethane cross-link) via an N<sup>1</sup>,O<sup>6</sup>-ethanoguanine

Received: January 3, 2014

Published: March 11, 2014

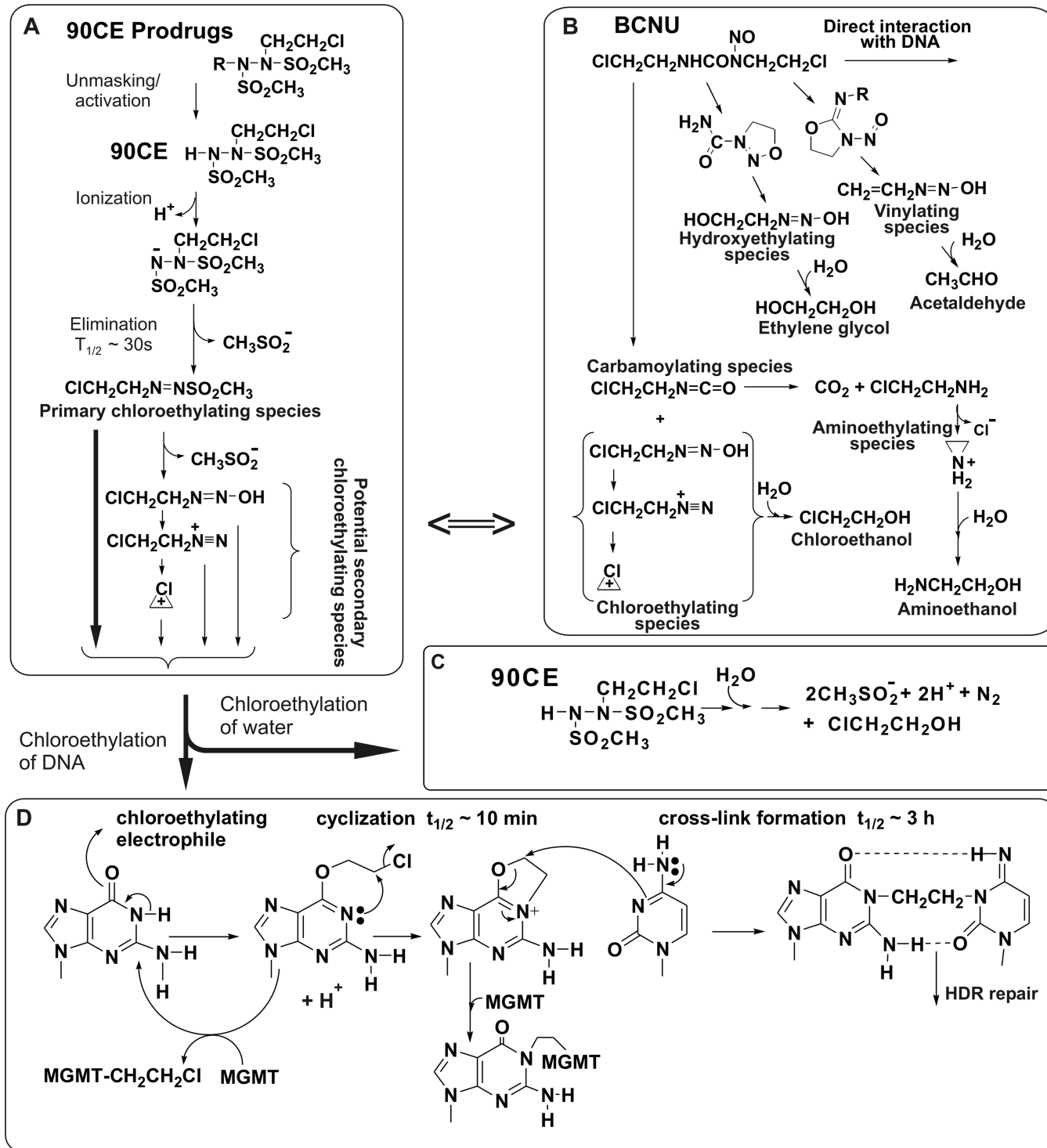


**Figure 1.** Summarizing scheme illustrating the generation of therapeutic guanine O-6 lesions and G-C ethane cross-links exploiting tumor cell DNA repair deficiencies by 90CE and prodrugs thereof and BCNU. (Panel A) The generation from 90CE and prodrugs thereof of primary and potential secondary chloroethylating species. (Panel B) The generation from BCNU of aminoethylating, carbamoylating, hydroxyethylating, and vinylating species not strongly associated with therapeutic activity, and the formation of therapeutic anticancer chloroethylating species which are potentially in common with the secondary chloroethylating species generated by 90CE. (Panel C) The overall stoichiometry for the generation of chloroethanol via the chloroethylation of water by 90CE via the primary or the secondary chloroethylating species. (Panel D) Scheme showing the major therapeutically relevant DNA lesions generated by oxophilic chloroethylating electrophiles and the cellular processes involved in their repair. Chloroethylation of the O-6 position of guanine results in the formation of O<sup>6</sup>-(2-chloroethyl)guanine. This lesion can be restored by MGMT or cyclize to form 1-(N<sup>3</sup>-cytosinyl)-2-(N<sup>1</sup>-guaninyl)ethane. This latter lesion can either react with the opposing cytosine to form a high cytotoxic G-C ethane cross-link or with MGMT preventing cross-link formation, but additional processes are required to complete the repair. Cells have a limited capacity to repair the resultant G-C ethane cross-links via HDR.

intermediate (Figure 1).<sup>7–9</sup> Selectivity for tumor cells arises from differentials between normal and tumor cells in their effective levels of MGMT, the resistance protein responsible for the repair of DNA O-6 guanine lesions, and in their ability to repair the resultant cross-links generated from lesions that evade restoration by MGMT.<sup>9–11</sup> Each MGMT molecule can only repair a single O-6 guanine lesion; therefore, the MGMT content correlates with sensitivity to agents of this type.<sup>8,9</sup> Few tumors are completely devoid of MGMT activity, but those that are exhibit high sensitivities to agents that generate guanine O-6 lesions among their repertoire of DNA damage.<sup>8</sup>

Once formed, the G-C ethane cross-link, which does not contain an O-6 linkage, cannot be repaired by MGMT.<sup>12</sup> However, cells can repair a limited number of G-C ethane cross-links, probably using homology directed repair (HDR).<sup>13</sup> As expected, cells possessing defective HDR show additional sensitivity to laromustine, and cells lacking both HDR and MGMT are hypersensitive to this agent.<sup>14</sup> A very small proportion of tumors are likely to possess both of these defects, but it is possible to screen for subsets of cancers that would likely exhibit exceptional sensitivity to 90CE prodrugs. Compared to BCNU (1,3-bis(2-chloroethyl)-1-nitrosourea), which generates a wide array of electrophiles, including carbamoylating species (Figure 1), a greater proportion of the overall cytotoxicity of 90CE appears to depend upon the O-6 chloroethylation of guanine. In support of this assertion, a ~22-fold differential in clonogenic LC<sub>90</sub> values was found between L1210 cell lines expressing and not expressing MGMT for 90CE, compared to only a ~2-fold differential for BCNU in the same matched cell line pair.<sup>15</sup> Furthermore, laromustine produces 100% cures in many MGMT-deficient *in vivo* tumor models and has a therapeutic index (LD<sub>50</sub>/ED<sub>50</sub>) against the L1210 leukemia of >8, more than double that of over 300 nitrosoureas tested.<sup>16,17</sup>

Electrophilic and nucleophilic species can be described as hard or soft, and this concept can be used to predict their reaction site preference.<sup>18</sup> Hard electrophiles have a high positive charge density and tend to react via S<sub>N</sub>1 reaction mechanisms with hard nucleophiles which have a high negative charge density. In contrast, soft electrophiles have a low charge density or are easily polarized and tend to react via S<sub>N</sub>2 reaction mechanisms with soft nucleophiles that have a low negative charge density or are easily polarized. The relative hardness and softness of electrophiles determines the spectrum of nucleophilic positions available in DNA for preferred reactions.<sup>18</sup> The DNA-backbone phosphate groups are the hardest nucleophilic sites in DNA, and the O-6 position of guanine is the hardest base centered site, while the N-7 position of guanine is the softest.<sup>18</sup> A single therapeutic alkylating agent can generate a wide array of lesions on sites of diverse hardness/softness in DNA because complex decomposition pathways can result in the production of many alkylating species with a wide range of hardness/softness and hence different and/or overlapping alkylation site preferences. This is the case with BCNU, which generates several potential chloroethylating species together with species that hydroxethylate, vinylate, aminoethylate, and carbamoylate.<sup>7,11,19–22</sup> While O-6 chloroethylation of guanine still dominates in terms of the anticancer activity of BCNU, it is a relatively minor product compared to alkylations on the N-7 or N-1 positions of DNA guanine.<sup>23</sup> 90CE was designed to generate a unique primary chloroethylating species (ClCH<sub>2</sub>CH<sub>2</sub>N=NSO<sub>2</sub>CH<sub>3</sub>), but this intermediate could potentially give rise to three other

secondary chloroethylating species (2-chloroethyldiazohydroxide, 2-chloroethyldiazonium, and chloronium ions) that are in common with those believed to be generated by BCNU (Figure 1).<sup>5,7</sup> Nevertheless, the pattern of DNA alkylation by 90CE appears to have a greater O-6 guanine to N-7 guanine alkylation bias under biologically relevant conditions and in *in vitro* and *in vivo* models than that of BCNU.<sup>7,9,16</sup>

We have previously studied the decomposition mechanism of 90CE in non-Pi and low Pi buffers;<sup>5</sup> under these conditions, 90CE appears to decompose in a relatively simplistic manner, as initially intended by design, to generate approximately two moles of methanesulfinate, one mole of nitrogen gas, and one mole of 2-chloroethanol, produced as a consequence of the chloroethylation of water (Figure 1). It was found that the rate determining step during the decomposition of 90CE and 1,2-bis(sulfonyl)-1-alkylhydrazines was the elimination of the N-1 sulfonyl moiety from the 1,2-bis(sulfonyl)-1-alkylhydrazine anion,<sup>5</sup> which in the case of 90CE results in the formation of the primary chloroethylating species ClCH<sub>2</sub>CH<sub>2</sub>N=NSO<sub>2</sub>CH<sub>3</sub> (Figure 1). Subsequently, we have found that in the presence of high concentrations of Pi, the alkylation of 4-(4-nitrobenzyl)-pyridine (4NBP) by 90CE was greatly increased. 4NBP is the most commonly used colorimetric reagent for determining alkylating activity, and the pyridine nitrogen which serves as the nucleophilic target in this molecule is a moderately soft site.<sup>24</sup> Thus, 4NBP would normally be expected to be poorly alkylated by 90CE, as is found in the absence of Pi. This Pi dependent change in character was not observed with 1,2-bis(methylsulfonyl)-1-methylhydrazine (KS90), the methylating analogue of 90CE. In view of the ubiquitous cellular presence of Pi, this interaction was further investigated, and a second decomposition pathway for 90CE has been elucidated. The implications of these findings in terms of future drug designs, tumor cell selectivity, agent toxicity, and possible novel resistance mechanisms are discussed.

## MATERIALS AND METHODS

**Caution:** Both 90CE and KS90 are potentially carcinogenic and mutagenic and should be handled carefully using personal protective equipment.

**Chemicals and Reagents.** 90CE was synthesized as previously described.<sup>25</sup> All other chemicals were purchased from the Sigma-Aldrich Chemical Co., St. Louis, MO, except where specified. Hoechst 33258 was obtained from Molecular Probes, Inc., Eugene, OR; HP $\beta$ CD, (2-hydroxypropyl)- $\beta$ -cyclodextrin was obtained from American Maize Products Company (1100 Indianapolis Boulevard, Hammond, IN).

**Test DNA Production and Isolation.** Murine L1210 leukemia cells were used as a source of DNA for DNA cross-linking assays. L1210 leukemia cell lines were grown in suspension culture in RPMI 1640 medium supplemented with 10% FBS in air/5% CO<sub>2</sub> at 37 °C. The cells were subcultured as required every 2–3 days. DNA was isolated using a Puregene DNA isolation kit (Genta Systems, Minneapolis, MN) using procedures recommended by the manufacturer. Isolated L1210 DNA was diluted to ~400 µg/mL with 5 mM Tris, 1 mM EDTA, and 1 mM Na<sub>3</sub>N<sub>3</sub> at pH 7.4 buffer, and stored at 4 °C until required.

**Effects of Pi Concentration on the Alkylation of 4NBP by 90CE and BCNU.** The alkylation of 4NBP by 90CE in the presence of various concentrations of Pi was studied using a method that is dependent upon the high pH aqueous stabilization of alkylated 4NBP using (2-hydroxypropyl)- $\beta$ -cyclodextrin (HP $\beta$ CD).<sup>24</sup> These experiments were performed using a 1.8 mL reaction volume. All buffers contained 20 mM Tris-HCl (pH 7.4) and various concentrations of potassium phosphate 0–200 mM (pH 7.4). 4NBP was added to give a final concentration of 1 mg/mL (close to its solubility at 37 °C) from a

50× stock solution in DMSO, and  $\alpha$ -thioglycerol (TG) was added as a competing nucleophile in some experiments to give final concentrations of either 1 or 20 mM from 100× aqueous stock solutions. The reactions were initiated by the addition of 200  $\mu$ M 90CE (100 mM stock solutions in DMSO) and incubated at 37 °C for 15 min. Some analogous experiments were performed using BCNU in place of 90CE with 20 h overnight incubations being utilized due to its more than 60-fold longer  $t_{1/2}$  time. The samples were assayed for 4NBP alkylation products by rapidly mixing equal volumes of the above reaction mixtures with 38% HP $\beta$ CD in 0.5 M KOH at room temperature and recording the absorbance at 635 nm within 1 min.

Aging experiments to follow the loss of the ability of 90CE to alkylate 4NBP under high Pi concentrations were performed in a very similar manner. The reaction was initiated by the addition of 200  $\mu$ M 90CE to 200 mM potassium phosphate buffer (pH 7.4) at 37 °C with very rapid mixing. One milliliter samples were then taken from this mixture and rapidly mixed with 20  $\mu$ L of 50 mg/mL of 4NBP in DMSO, 0, 30, 60, 90, 120, and 300 s after reaction initiation, and incubated for a further 15 min. The samples were then assayed for 4NBP alkylation as described above.

**Alkylation of 2-Mercapto-5-nitropyridine (MNP).** MNP is a highly chromophoric thiol/thiolate at physiological pH values, absorbing with a  $\lambda_{\text{max}}$  at 389 nm.<sup>26</sup> In these experiments, observations were made at 440 nm because at this wavelength, the extinction coefficient is still substantial, and derivatization of the thiol/thiolate causes a complete rather than a partial bleaching of the absorbance. MNP was generated *in situ* from 2,2'-dithiobis(5-nitropyridine) by reduction with thioglycerol (TG). To a 60  $\mu$ M DTBNP solution (10 mM stock in DMSO) in 200 mM potassium phosphate buffer (pH 7.4, 37 °C), a limiting quantity of 100  $\mu$ M TG (10 mM stock in H<sub>2</sub>O) was added; this should convert ~50  $\mu$ M of the DTBNP to ~100  $\mu$ M of MNP, exhausting the TG and leaving MNP as essentially the only thiol present. This assumption was confirmed by observing an equivalent increase in absorption at 440 nm upon adding a 100 molar-fold excess of TG to 50  $\mu$ M DTBNP. The absorbance of 100  $\mu$ M MNP at 440 nm was ~0.775 AU and was attained within a few minutes of the addition of 100  $\mu$ M TG at 37 °C and remained stable thereafter at this level. Addition of excess 90CE (500  $\mu$ M) fully bleached the MNP absorbance in <1 min. This method for producing MNP was used to follow the extent and kinetics of alkylation/bleaching of MNP upon the addition of limiting aliquots of 90CE in 200 mM potassium phosphate buffer.

**Effects of Anions/Solutes on the 90CE Decomposition Pathway.** To examine the effects of anions/solutes other than phosphate on the generation of soft electrophilic species from 90CE, identical experiments were performed in 20 mM Tris-HCl buffer (pH 7.4, 37 °C) containing 100  $\mu$ M MNP (generated *in situ* as described) in which the buffer was supplemented with various solutes (pH adjusted to 7.4) at 50 mM. The bleaching of MNP was followed after the addition of 100  $\mu$ M 90CE over 5 min (50 mM Pi results in a submaximal effect). In the case of ATP, some experiments were also performed in the presence of a 1.05-fold molar excess of MgCl<sub>2</sub>.

**Effects of Pi and TG on DNA Cross-Link Generation by 90CE.** Reaction mixtures had a final total volume of 40  $\mu$ L and were made up in 5 mM Tris-HCl, 1 mM EDTA, and 1 mM NaN<sub>3</sub> buffer (pH 7.4) and contained L1210 leukemia DNA (120  $\mu$ g/mL), various final concentrations of Pi (0–100 mM), and  $\pm$ 20 mM TG. The reactions were initiated by the addition of 90CE to give a final concentration of 100  $\mu$ M (4  $\mu$ L of 1.0 mM 90CE in 1.0 mM HCl). These samples were then incubated for 15 min at 37 °C, then diluted by the addition of 560  $\mu$ L of 5 mM Tris-HCl, 1 mM EDTA, and 1 mM NaN<sub>3</sub> (pH 8.0) buffer to give a total volume of 600  $\mu$ L. At this point, these DNAs then contained a monoadduct cross-link precursor ( $O^6$ -(2-chloroethyl)-guanine and  $N^1,O^6$ -ethanoguanine) but insignificant cross-links. These samples were then incubated at 50 °C for a further 3 h to allow the monoadducts sufficient time to fully react with the complementary strand and generate DNA interstrand cross-links. From these samples, 200  $\mu$ L was used for each cross-linking level determination. The level of DNA cross-linking was then determined using a modification of a previously described assay.<sup>13,27</sup> This assay is based upon the fact that

upon rapid cooling thermally denatured DNA containing one or more covalent interstrand cross-links rapidly renatures, yielding a highly fluorescent complex with H33258 dye. The 200  $\mu$ L aliquots of L1210 DNA containing various levels of interstrand cross-links were added to 1.5 mL of 5 mM Tris-HCl, 1.0 mM EDTA, and 1.0 mM NaN<sub>3</sub> buffer (pH 8.0) containing 0.1  $\mu$ g/mL of H33258, heated to 100 °C for 3 min, then plunged into a water bath at room temperature for 3 min. Fluorescence measurements were taken before the heating phase and after the 3 min chill using a Hoefer Scientific Instruments TKO 100 fluorometer, and the fraction of the DNA molecules that were cross-linked (i.e., that contained at least one cross-link per DNA molecule) and the average number of cross-link moieties per DNA molecule calculated assuming a Poisson distribution as previously described.<sup>13</sup>

**Decomposition/Reaction Kinetics of 90CE in the Absence of Pi by H<sup>+</sup> Generation.** The decomposition/reaction of 90CE involves the formation of a strong acid (methanesulfonic acid, pK<sub>a</sub> ~ 2) and thus can be followed using protonometric assays. We utilized a simple colorimetric assay that relies upon the measurement of the relatively linear change in absorption at 560 nm of phenol red that occurs in proportion to the generation/addition of small quantities of hydrogen ions when a weakly buffered solution of this pH indicator is subjected to incremental acidification over a narrow pH range ( $\Delta\text{pH} < 0.1$  unit) close to the pK<sub>a</sub> values of the buffer/indicator components.<sup>28</sup> Using a 20  $\mu$ g/mL solution of phenol red in 2 mM Tris-HCl buffer, the absorbance at 560 nm was followed at an initial pH value of 7.4 at 20 and 37 °C upon the addition of 50  $\mu$ M 90CE (5  $\mu$ L/mL of 10 mM 90CE in DMSO). The assay mixtures were sealed with parafilm in 1 mL cuvettes to minimize changes in pH due to CO<sub>2</sub> exchange and brought to the appropriate temperature prior to the addition of agent via injection through the parafilm and rapid mixing.

**Decomposition/Reaction Kinetics of 90CE in the Presence and Absence of Pi by the Generation of UV Absorbing Species.** Decomposition/reaction kinetics of 90CE (100  $\mu$ M) were followed at both 20 and 37 °C in 200 mM potassium phosphate (pH 7.4) and 20 mM Tris-HCl (pH 7.4) by recording the appearance of UV absorbing material at 240 nm after the addition of 10  $\mu$ L/mL of a 10 mM 90CE solution in DMSO. Because of the temperature dependence of the dissociation constants of the buffer constituents, in particular that of Tris-HCl, the buffer pH values must be set at the appropriate assay temperature.

**Kinetics of the Loss of the Ability of 90CE to Generate DNA O-6 Guanine Chloroethylating Electrophiles upon Aging.** The loss of the ability of 90CE to chloroethylate the O-6 position of DNA guanine was examined by following the exhaustion of DNA cross-linking capability versus time at pH 7.4 and 37 °C in 20 mM Tris buffer. To 500  $\mu$ L of 20 mM Tris buffer (pH 7.4 at 37 °C), 100  $\mu$ M 90CE was added (10  $\mu$ L of 10 mM 90CE in DMSO) to initiate electrophile generation; at various times after initiation and mixing (0, 30, 60, 90, 120, and 300 s), aliquots (12  $\mu$ L) were withdrawn and mixed with an equal volume of L1210 DNA 400  $\mu$ g/mL in 5 mM Tris, 1 mM EDTA, and 1 mM NaN<sub>3</sub> (pH 7.4) buffer and rapidly mixed. These mixtures were then incubated for 15 min at 37 °C, diluted to a volume of 600  $\mu$ L with 5 mM Tris, 1 mM EDTA, and 1 mM NaN<sub>3</sub> (pH 8.0) buffer then incubated at 50 °C for a further 3 h. The level of DNA cross-linking and the number of cross-link moieties per DNA molecule were then measured and calculated as described above.

**Determination of 2-Chloroethanol.** Chloroethanol is generated as a consequence of the chloroethylation of water by 90CE. Water is a particularly good trapping agent since it is present at a concentration of ~55 M, which results in it sequestering the vast majority of the harder electrophiles generated.<sup>13</sup> Since 2-chloroethanol lacks any strong spectroscopic features and is relatively unreactive, it is necessary to transform it into a chromophoric derivative. Therefore, the 2-chloroethanol was oxidized to its corresponding aldehyde using *Pichia pastoris* alcohol oxidase (AO), a relatively nonspecific enzyme which oxidizes short-chain, linear aliphatic alcohols to their respective aldehydes.<sup>29,30</sup> The resultant aldehyde was then reacted with 2,4-dinitrophenylhydrazine (2,4-DNPH) to generate a hydrazone product which was quantified by HPLC. To 0.5 mL samples of pH 7.4 buffers containing various concentrations of Pi (0–200 mM), 1.0 mM 90CE

(5  $\mu$ L of 100 mM 90CE in DMSO) was added. The 0 mM Pi buffer experiments contained 20 mM Tris (pH 7.4) to allow the decomposition to fully proceed, which would normally slow substantially as the pH fell, due to the liberation of methanesulfonic acid. These mixtures were incubated for 5 min at 40 °C, then diluted 10-fold with distilled H<sub>2</sub>O. To 0.5 mL of this diluted mixture, 10 unit/mL of AO was added and the mixture incubated for 30 min at 40 °C in sealed tubes with occasional shaking to maintain aeration. Aliquots (0.5 mL) were then mixed with an equal volume of a 0.4% solution of 2,4-DNPH in CH<sub>3</sub>CN and 50  $\mu$ L of 1 M HClO<sub>4</sub>, and the mixture incubated at 40 °C for 5 min and then assayed directly by HPLC. The HPLC protocol utilized a 250 mm × 4.6 mm Varian Microsorb 100-5 C-18 reverse phase column (Varian Inc., Lake Forest, California, USA) and a constant composition buffer (52.5% CH<sub>3</sub>CN and 47.5% 30 mM potassium phosphate, pH 5.4) at a flow rate of 0.8 mL/min. The hydrazone eluted at ~16.3 min and was monitored at 370 nm. All HPLC measurements were performed using a Beckman 127P solvent module and a Beckman 168 UV/vis detector (Beckman, Fullerton, CA, USA). This assay gave good linearity in the test range using authentic 2-chloroethanol samples and was not significantly affected by the initial buffer composition. The limit of 2-chloroethanol detection using this method was ~1  $\mu$ M. Assays were compared with identical reagent blanks containing all components except 90CE.

**Determination of Acetaldehyde.** Acetaldehyde yields were determined using a protocol identical to that used for measuring 2-chloroethanol, except that the addition of and incubation with AO were not required. The assay was calibrated using authentic acetaldehyde standards, and the resultant hydrazone eluting at 14.9 min gave a linear AUC (area under the curve) for the resultant hydrazone peak versus the initial concentration of acetaldehyde. The AUC of the hydrazone product peak over that of DMSO controls was used to calculate the acetaldehyde yields by comparison with authentic standards. Assays were compared with identical reagent blanks containing all components except 90CE. The limit of detection was approximately 1  $\mu$ M.

**Determination of Ethylene Glycol.** Ethylene glycol was measured in a manner similar to that used with 2-chloroethanol, except that a longer 60 min incubation with AO was utilized to oxidize the ethylene glycol to glyoxal since ethylene glycol is a poorer substrate for this enzyme. Even with this longer incubation time, the oxidation was not complete, and the yield of glyoxal was approximately 50% at all concentrations (based upon comparisons with authentic glyoxal samples). In addition, the hydrazone generated from glyoxal required the use of an increased CH<sub>3</sub>CN concentration (75% CH<sub>3</sub>CN and 25% 30 mM potassium phosphate, pH 5.4) in the HPLC protocol compared to the previous method to avoid excessively long elution times. Under these revised HPLC conditions, the hydrazone product eluted at ~9 min. Ethylene glycol standards gave a linear AUC for the resultant hydrazone peak versus the initial concentration of ethylene glycol. The AUC of the glyoxal hydrazone product peak over that of DMSO controls was used to calculate the ethylene glycol yield by comparison with authentic standards. The limit of detection was approximately 3  $\mu$ M.

**Chloride Determination.** The generation of free chloride during the decomposition of 90CE in buffers containing various concentrations of Pi was assayed using a modification of the method of Jörg and Bertau.<sup>31</sup> This is a highly sensitive colorimetric assay based on the formation and strong absorbance of [FeCl]<sup>2+</sup> at  $\lambda_{\text{max}}$  340 nm. This cation is very stable under highly acidic conditions. For these studies, all buffers must be completely free of chloride anions. A 200 mM Tris-acetate buffer (pH 7.4) (produced using Tris free base and glacial acetic acid) and a 200 mM potassium phosphate buffer (pH 7.4) (produced using KH<sub>2</sub>PO<sub>4</sub> and KOH) were combined in various proportions to generate chloride free buffers with Pi concentrations between 0 and 200 mM. The use of DMSO resulted in some increased background values with this assay. This was circumvented by formulating 0.5 M 90CE stock solutions in hydroxyacetone (acetol) for these experiments. Two additional problems were encountered, one associated with the determination of chloride in the presence of high Pi levels in an Fe<sup>3+</sup> based assay and a second due to an additional

background generated from nonchloride 90CE decomposition products (discovered by utilizing KS90 as a control agent, with KS90 being a 90CE analog in which the chloroethyl moiety is replaced by a methyl group and therefore unable to liberate chloride). The first problem was resolved by precipitation of the Pi using Ca(NO<sub>3</sub>)<sub>2</sub> prior to the assay. The second problem was negated by splitting each sample into two, removing the chloride from one portion by utilizing silver acetate precipitation and using this chloride free counterpart as the reagent blank against which the second portion was measured.

The final assay protocol was as follows. To 2 mL samples of buffers containing various levels of Pi, formulated as described above, 40  $\mu$ L of 0.5 M 90CE dissolved in acetol was added to give a final 90CE concentration of 10 mM. This mixture was then incubated for 20 min at 37 °C to allow for complete decomposition. These samples were then diluted 10-fold with distilled water and 0.1 mL of saturated 1.6 M Ca(NO<sub>3</sub>)<sub>2</sub> solution added per mL and the precipitate removed by centrifugation. The supernatants were then split into two portions and one-half treated with 40  $\mu$ L/mL of 50 mM silver acetate and the other with 40  $\mu$ L/mL of distilled water. These samples were then centrifuged to remove any precipitate and 0.5 mL samples of supernatant mixed with an equal volume of 40 mM Fe(NO<sub>3</sub>)<sub>3</sub> in 50% perchloric acid, and the absorbance of the experimental sample measured at 340 nm versus its chloride depleted counterpart. This assay was linear using chloride standards and chloride spiked experimental controls independent of the buffer Pi concentration.

**Determination of Methanesulfonic Acid Yields during 90CE Decomposition.** Methanesulfonic acid was assayed by a modification of the method of Babbs and Gale,<sup>32</sup> which is based upon the reaction of an aromatic diazonium salt (Ar-N=N<sup>+</sup>), in this case, Fast Blue BB salt with methanesulfonic acid to produce a chromophoric diazosulfone derivative (Ar-N=N-SOOCCH<sub>3</sub>), which is highly hydrophobic and thus can be selectively extracted into an organic solvent and determined spectrophotometrically. Ten microliter aliquots of 100 mM 90CE in DMSO were added to 1.0 mL samples of pH 7.4 buffers containing various Pi contents (0–200 mM) to give a final 90CE concentration of 1 mM. The 0 mM Pi buffer experiments contained 20 mM Tris-HCl buffer (pH 7.4) to allow the decomposition to fully proceed, which would normally slow substantially as the pH fell due to the liberation of methanesulfonic acid. These mixtures were incubated for 5 min at 37 °C to allow for a complete decomposition/reaction, and then aliquots were diluted 40-fold with 500 mM NaH<sub>2</sub>PO<sub>4</sub>/H<sub>3</sub>PO<sub>4</sub> (pH 2.2) containing 1 part in 80 of saturated Fast Blue BB salt solution in 500 mM NaH<sub>2</sub>PO<sub>4</sub>/H<sub>3</sub>PO<sub>4</sub> (pH 2.2). These mixtures were allowed to react at 40 °C for 10 min in the dark. An equal volume (0.8 mL) of *n*-octanol pre-equilibrated with 500 mM NaH<sub>2</sub>PO<sub>4</sub>/H<sub>3</sub>PO<sub>4</sub> was then added and the tubes vigorously shaken for 2 min en masse; the samples were then centrifuged at 10,000g for 120 s, and the upper octanol layer was separated and the absorbance measured at 460 nm versus a reagent blank within 5 min. Calibration curves were generated using solutions of authentic sodium methanesulfinate at concentrations of 0.0, 0.5, 1.0, 1.5, 2, and 3 mM in buffers with various Pi contents (0–200 mM), and a linear response (absorbance 460 nm versus methanesulfinate concentration) was observed that was independent of the Pi concentration in the initial samples.

**Trapping and Isolation of a Novel Thiophilic Electrophile Species.** The strongly absorbing thiol MNP produced by reducing DTBMP was used as a convenient electrophile trapping agent suitable for the separation by HPLC. The HPLC protocol utilized a 250 mm × 4.6 mm Varian Microsorb 100-5 C-18 reverse phase column (Varian Inc.) and elution with an unbuffered CH<sub>3</sub>CN/H<sub>2</sub>O solvent system, starting with 5% acetonitrile for 5 min followed by a 5–50% CH<sub>3</sub>CN linear gradient over the subsequent 30 min. After this point, the concentration of CH<sub>3</sub>CN was maintained at this level for 5 min, then returned to the starting concentration over an additional 5 min. Absorbance was monitored at 340 nm using a Beckman 168 UV/vis detector; 340 nm was chosen because the strong absorption of the 5-nitropyridine moiety is largely independent of the derivatization or oxidation state of the attached thiol group at this wavelength. The reduced thiol (MNP) and oxidized disulfide dimer (DTBMP) elute at ~5 and ~38 min, respectively. The reaction protocol was as follows: 1

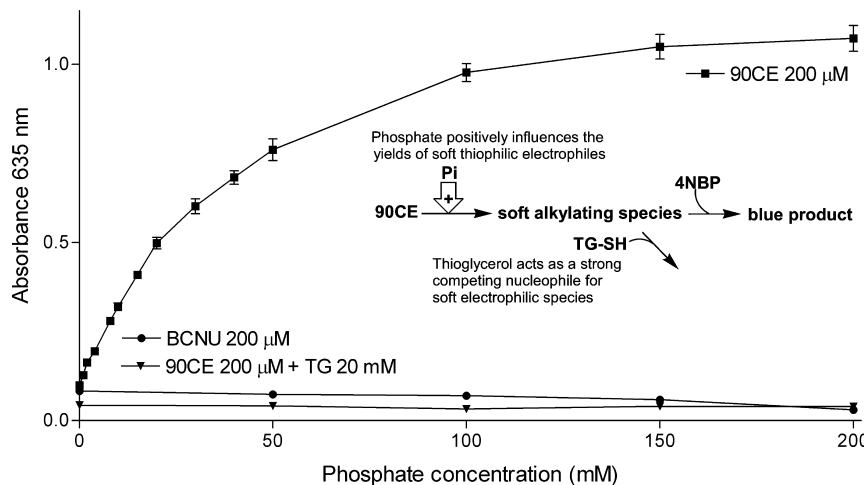


**Figure 2.** Effect of Pi concentration on the preference of 90CE and BCNU for 4NBP. Reactions containing either 200  $\mu$ M 90CE ( $\pm$ 20 mM TG) or 200  $\mu$ M BCNU and 1 mg/mL of 4NBP (4.7 mM) in 20 mM Tris-HCl buffer (pH 7.4) containing various concentrations of Pi (pH 7.4) samples were reacted for either 15 min at 37 °C for 90CE or overnight at 37 °C for BCNU due to its >60-fold longer  $t_{1/2}$ . The resultant level of 4NBP alkylation was then determined by measuring the absorbance at 635 nm versus a reagent blank after mixing samples with an equal volume of 38% HP $\beta$ CD dissolved in 0.5 M KOH. (■) 200  $\mu$ M 90CE in the absence of TG; (▼) 200  $\mu$ M 90CE in the presence of 20 mM TG; and (●) 200  $\mu$ M BCNU in the absence of TG. All values are the result of at least 3 determinations  $\pm$  SE.

mM DTBNP in 200 mM K<sub>2</sub>HPO<sub>4</sub> was reduced to MNP by the addition of 2 mM thioglycerol to generate  $\sim$ 2 mM MNP in a high Pi buffer environment. After a few minutes of gentle shaking at room temperature to ensure that the reduction was complete, an aliquot of 100 mM 90CE in DMSO was added to give a final concentration of 2 mM 90CE. This mixture was incubated for 4 min at 37 °C, centrifuged at 10,000g for 1 min, then diluted 10-fold with distilled water and immediately analyzed by HPLC. This reaction sequence is easily followed by the eye, as reduction to MNP caused the sample to develop a strong yellow color, which is then largely discharged over a few minutes upon alkylation by 90CE. Under these reaction conditions, only one new MNP/90CE derived major product, eluting as a broad tailing peak (10–13 min, peak 11.6 min), was observed. A similar experiment was performed at four times these concentrations of MNP and 90CE and the alkylated product peak collected for analysis by LCMS.

**LCMS of Trapped Adduct.** The alkylated product prepared, separated, and collected as described above was analyzed by mass spectroscopy using a chromatographic system consisting of an Agilent 1200 series HPLC system, including a binary pump (Model G1312B), a vacuum degasser (Model G1379B), an autosampler (Model G1367C), and a column oven (Model G1316B). The mass spectrometer was an Applied Biosystems Sciex 4000 Q-trap mass spectrometer (Applied Biosystems Sciex; Foster, CA). Data acquisition was carried out by Analyst 1.4.2 software on a Dell computer. A declustering potential of 50 V, excitation energy of 100 V, and a collision energy of 10 V were utilized.

## RESULTS AND DISCUSSION

Previous studies, in the absence of high Pi concentrations, demonstrated that the initial elimination of the N-1 sulfinate moiety was the rate determining step in the decomposition of 1,2-bis(sulfonyl)-1-alkylhydrazines (Figure 1 panel A) as measured by hydrogen ion production.<sup>5</sup> This time course also corresponded to the loss of biological activity upon agent aging.<sup>5</sup> The instantaneous release of the first mole of protons represents the ionization of the acidic N-2 hydrogen and cannot reflect the elimination of the N-1 sulfinate acid moiety from the un-ionized parental 1,2-bis(sulfonyl)-1-alkylhydrazine because the  $t_{1/2}$  for the first order release of the second mole of protons decreases with the increasing leaving group ability of the N-1 sulfinate moiety, and this could not occur if the N-1 sulfinate

moiety had already left the molecule.<sup>5</sup> The release of the second mole of protons occurs upon nucleophile alkylation by the primary oxophilic alkylating species RN=NSO<sub>2</sub>CH<sub>3</sub> (e.g., Figure 1 panel D) or secondary alkylating species derived from these. This biphasic release of two moles of hydrogen ions is observed during the decomposition of both methylating and chloroethylating analogues in a Pi free or low Pi buffers.<sup>5</sup> In Tris-HCl buffer, both KS90 and 90CE poorly alkylated 4NBP as would be expected for generators of relatively hard electrophiles. However, in 200 mM Pi buffer, the behavior of 90CE changed markedly, and a > 10-fold increase in the alkylation of 4NBP was observed. We therefore investigated the Pi concentration dependence of the alkylation of 4NBP (1 mg/mL,  $\sim$  4.7 mM) by 200  $\mu$ M 90CE over a 0–200 mM Pi concentration range (Figure 2). The presence of Pi resulted in a marked, but saturable, concentration dependent increase in 4NBP alkylation, with approximately 30 mM Pi eliciting a half-maximal effect under these conditions. The inclusion of 20 mM TG, as a competing soft nucleophile, decreased the alkylation of 4NBP at the highest Pi concentration by >96%. The addition of 1 mM TG was almost as effective, resulting in an  $\sim$ 90% reduction in 4NBP alkylation at 200 mM Pi (data not shown). Thus, the generated electrophile must be extremely soft in nature since only 1 mM 4NBP by  $\sim$ 90%. This very strong thiol preference is more reminiscent of a Michael addition reaction than the reaction of a nucleophile with a carbonium ion or highly polarized alkyl group. In comparison, BCNU at an equivalent concentration poorly alkylated 4NBP over a 0–200 mM Pi concentration range, and this NBP alkylation was marginally decreased rather than greatly increased at higher Pi concentrations (Figure 2), probably due to some alkylation of Pi. In addition, no Pi dependent increase in thiol preference was observed with BCNU (data not shown). Since 90CE can potentially generate three secondary chloroethylating species which are in common with the hard oxophilic chloroethylating species proposed for BCNU (Figure 1, panel B),<sup>5,7</sup> these findings imply that the Pi dependent increase in soft nucleophile preference seen with 90CE does not involve

these secondary chloroethylating species (Figure 1, panel A) but a component unique to 90CE.

In view of the Pi concentration dependent increase in the generation of soft thiophilic alkylating species with increasing Pi concentration from 90CE, we decided to examine the effects of Pi concentration on the formation of DNA interstrand cross-links which are dependent upon the generation of hard oxophilic chloroethylating electrophiles. DNA interstrand cross-link formation is of particular importance since it is crucial to the mode of action of 90CE prodrugs. It can be seen (Figure 3) that increasing the Pi concentration results in a

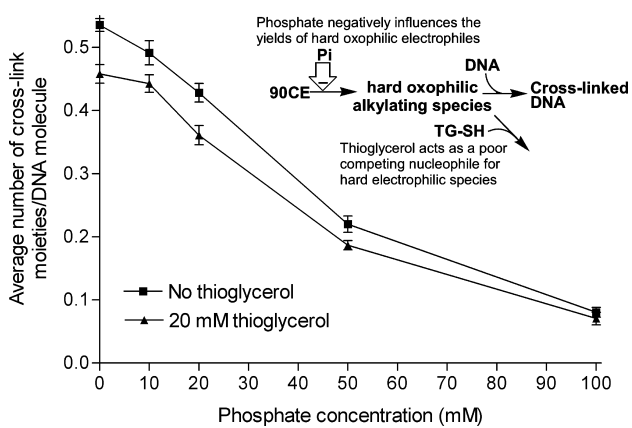


**Figure 3.** Effects of Pi concentration on the average number of cross-link moieties generated per DNA molecule (reaction concentration 120  $\mu\text{g}/\text{mL}$  of L1210 DNA) by 100  $\mu\text{M}$  90CE at pH 7.4 in the presence and absence of 20 mM TG as a competing nucleophile. (■) Average number of cross-link moieties generated per DNA molecule in the absence of TG; and (▲) average number of cross-link moieties generated per DNA molecule in the presence of 20 mM TG. All values are the result of at least 3 determinations  $\pm$  SE.

progressive decrease in the yield of DNA cross-linking moieties per DNA molecule and that the electrophiles responsible for generating these lesions are hard oxophilic electrophiles that are resistant to thiol interception since 20 mM TG only decreased the yields ~15%. Only a very small proportion of the oxophilic chloroethylating electrophiles generated react with the O-6 position of DNA guanine since the bulk chloroethylate water,<sup>13</sup> which is present at ~55 M, to generate 2-chloroethanol (Figure 1, panel C). This is especially true for hard oxophilic chloroethylating species, which have a strong preference for water-like nucleophiles.<sup>18</sup> However, it is expected that water in the absence of competing favored nucleophiles, due to its high concentration, would also trap the majority of any generated soft chloroethylating species as 2-chloroethanol. Therefore, we looked at the production of 2-chloroethanol versus Pi concentration to ascertain the changes occurring in the overall yields of chloroethylating electrophiles (Figure 4, panel A). A large decrease in chloroethanol production from ~83% to ~17% over a Pi concentration range of 0–200 mM was observed. This change approximately parallels the decrease seen in DNA cross-link formation and is the inverse of the increase observed in soft thiophilic alkylators in the 4NBP alkylation experiments. The corresponding decrease in chloroethanol production suggested that the soft thiophilic alkylator was not a chloroethylating species. The reduction in 2-chloroethanol yields could mean that the chlorine was lost as chloride or remained as part of a different species. We therefore measured chloride release and found that ~80% of the total chlorine was liberated as chloride under high Pi conditions (Figure 4, panel A). This finding confirmed that the chlorine was largely lost in the Pi catalyzed pathway and was no longer part of the donated electrophile moiety. It was thought that the loss of chloride by elimination or by a hydrolytic mechanism could possibly lead to either vinylating or hydroxyethylating species, respectively. Acetaldehyde and ethylene glycol are formed by the vinylation

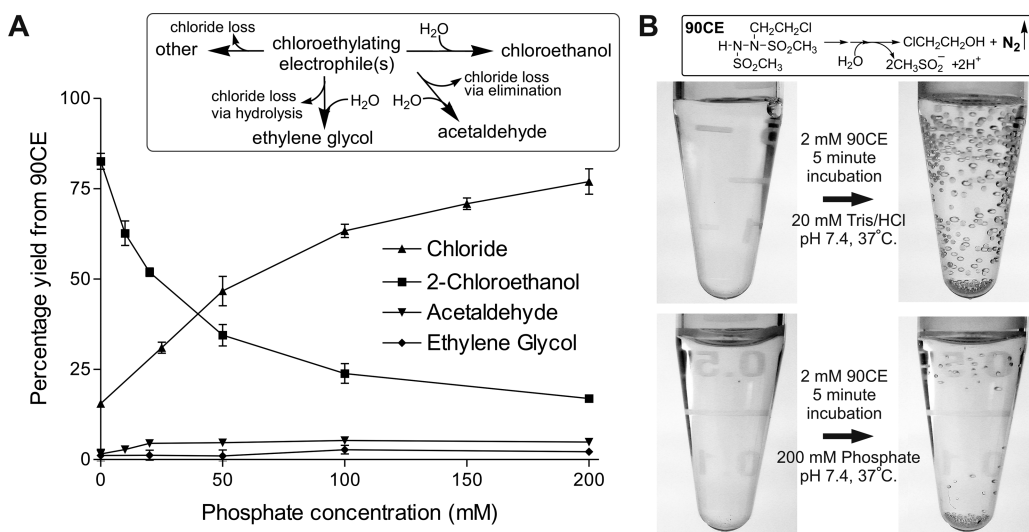


**Figure 4.** Effects of Pi concentration on the yields of 2-chloroethanol, acetaldehyde, ethylene glycol, and chloride anions (panel A), and nitrogen gas evolution from 90CE (panel B) at pH 7.4 and 37 °C. Panel A, (■) 2-chloroethanol, (▼) acetaldehyde, (◆) ethylene glycol, and (▲) chloride anions. All values are the result of at least 3 determinations  $\pm$  SE. (Panel A, insert) Potential fates for the chloroethylating species generated. The experimental data indicate that the formation of ethylene glycol and acetaldehyde are insufficient to account for the decreases in chloroethanol and increases in chloride formation observed under high Pi concentration conditions and that some other processes must account for these differences. (Panel B) Photographs taken just after the addition of 2 mM 90CE (upper and lower left-hand images) to microcentrifuge tubes containing either 20 mM Tris-HCl (upper row) or 200 mM potassium phosphate (lower row) buffers at pH 7.4, and after 5 min of incubation at 37 °C (upper and lower right-hand images), note the large decrease in nitrogen evolution under high phosphate conditions.

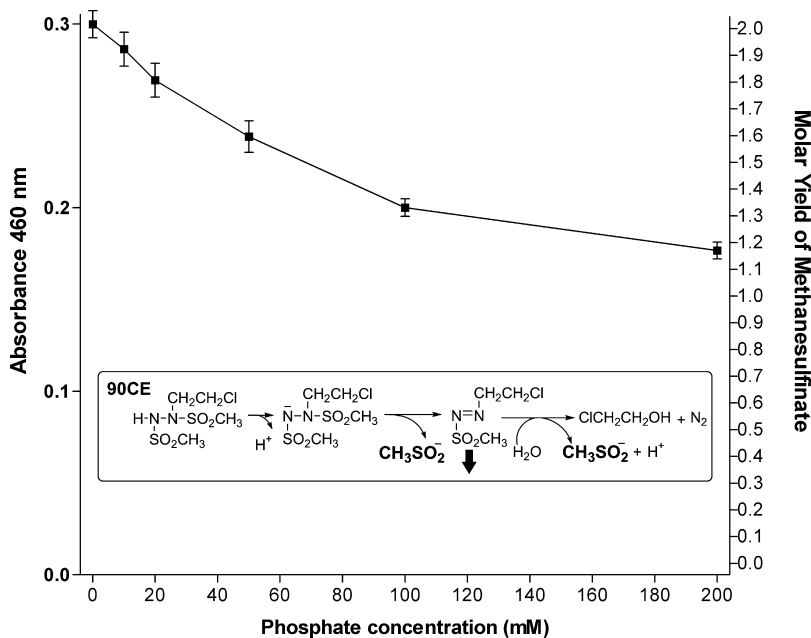


**Figure 5.** Effects of Pi concentration on the yields of methanesulfinate formed during the decomposition of 90CE. One millimolar solutions of 90CE were decomposed at 37 °C and pH 7.4 for 10 min in buffers containing various concentrations of Pi. These samples were derivatized with the aromatic diazonium dye Fast Blue to give the octanol soluble highly chromophoric diazosulfone derivative. The diazosulfone was separated into octanol and the absorbance measured at 460 nm versus a reagent blank (identical except for the absence of 90CE). All values are the result of at least 3 determinations  $\pm$  SE. (Insert) Decomposition scheme illustrating the generation of 2 mols of methanesulfinate per mol of 90CE in the absence of Pi, with the downward arrow representing a potential decomposition pathway branch point in the presence of Pi retaining a methanesulfinate moiety and both nitrogen atoms.

and hydroxyethylation of water, respectively, and can be generated in quite high yields by BCNU via decomposition pathways involving chloride loss (Figure 1, panel B).<sup>33</sup> For this reason, we assayed for the generation of these two chlorine-free two-carbon atom species during the decomposition of 90CE. At 200 mM Pi, the highest level tested, the yields of acetaldehyde and ethylene glycol were approximately 5% and 2%, respectively (Figure 4, panel A). These yields combined were insufficient in quantity to account for the large decrease in the yields of 2-chloroethanol (~83% to ~17%) between 0 mM Pi and 200 mM Pi, respectively (Figure 4 panel A). In previous studies following the decomposition of gram quantities of KS90,<sup>5</sup> both the volume and composition of the gas liberated were determined; and very close to a mole equivalent of nitrogen was found to be released during KS90 decomposition. While it is difficult to quantify and analyze microliter volumes of gas liberated during the decomposition of small quantities of dilute aqueous solutions of 90CE, at decomposition concentrations of  $\sim$ 1 mM or greater gas bubbles can be observed nucleating on the vessel's walls. We therefore quantified the bubble formation number during the decomposition of 2 mM solutions of 90CE in both Tris-HCl and 200 mM potassium phosphate and noted a >80% reduction in bubble numbers under high Pi conditions (Figure 4, panel B). This observation implied that the volume of gas liberated under high Pi conditions was also significantly reduced. The apparent failure of the bulk of the 90CE, under high Pi conditions, to liberate either the two carbon alkylating moiety as chloroethanol, acetaldehyde, or ethylene glycol and the hydrazine derived nitrogen, suggested that the molecule failed to fully fragment under these conditions. Consequently, we determined the effects of Pi concentration on the liberation of methanesulfinate during the decomposition of 90CE (Figure 5). The quantity of

methanesulfinate was found to be reduced from  $\sim$ 2 to  $\sim$ 1.2 mols per mol of 90CE under high Pi conditions. This finding is consistent with  $\sim$ 80% of the 90CE failing to fully fragment after the initial elimination of the N-1 methanesulfinate moiety, thus liberating a single mole of methanesulfinate instead of two at the highest concentrations of Pi. A small proportion ( $\sim$ 17%) of the 90CE appeared to decompose, liberating chloride even in the absence of Pi in the 200 mM Tris-acetate buffer used in the chloride assay. If this proceeded by the 1 mol of methanesulfinate route, one would expect 1 mol of 90CE to liberate a maximum of  $\sim$ 1.83 mols of methanesulfinate rather than 2 mols. This discrepancy could be due to a minor decomposition pathway(s) where both the chloride and second methanesulfinate are lost in the absence of Pi (potential minor pathway A, see later), a small Pi-like effect of the 200 mM Tris-acetate buffer used in the chloride determinations (see later), or an inaccuracy in the methanesulfinate standards due to hygroscopicity of the sodium salt used, or a combination of these possibilities.

Differences in the overall kinetics of alkylation by 90CE reacting via hard oxophilic or soft thiophilic alkylating species could arise from the change in the decomposition pathway since this could be accompanied by a change in the rate determining step. Furthermore, soft alkylating species could be expected to persist for longer time periods in aqueous solution and potentially extend the time course of alkylation in the absence of preferred nucleophiles or in the presence of rate limiting nucleophile concentrations. Therefore, the kinetics of the following processes were measured and compared: the kinetics of the release of the second mole of hydrogen ions (0 mM Pi), bleaching of MNP (200 mM Pi), and the generation of UV absorbing species (200 mM Pi), together with the loss of the ability of 90CE to produce DNA cross-link moieties (0 mM

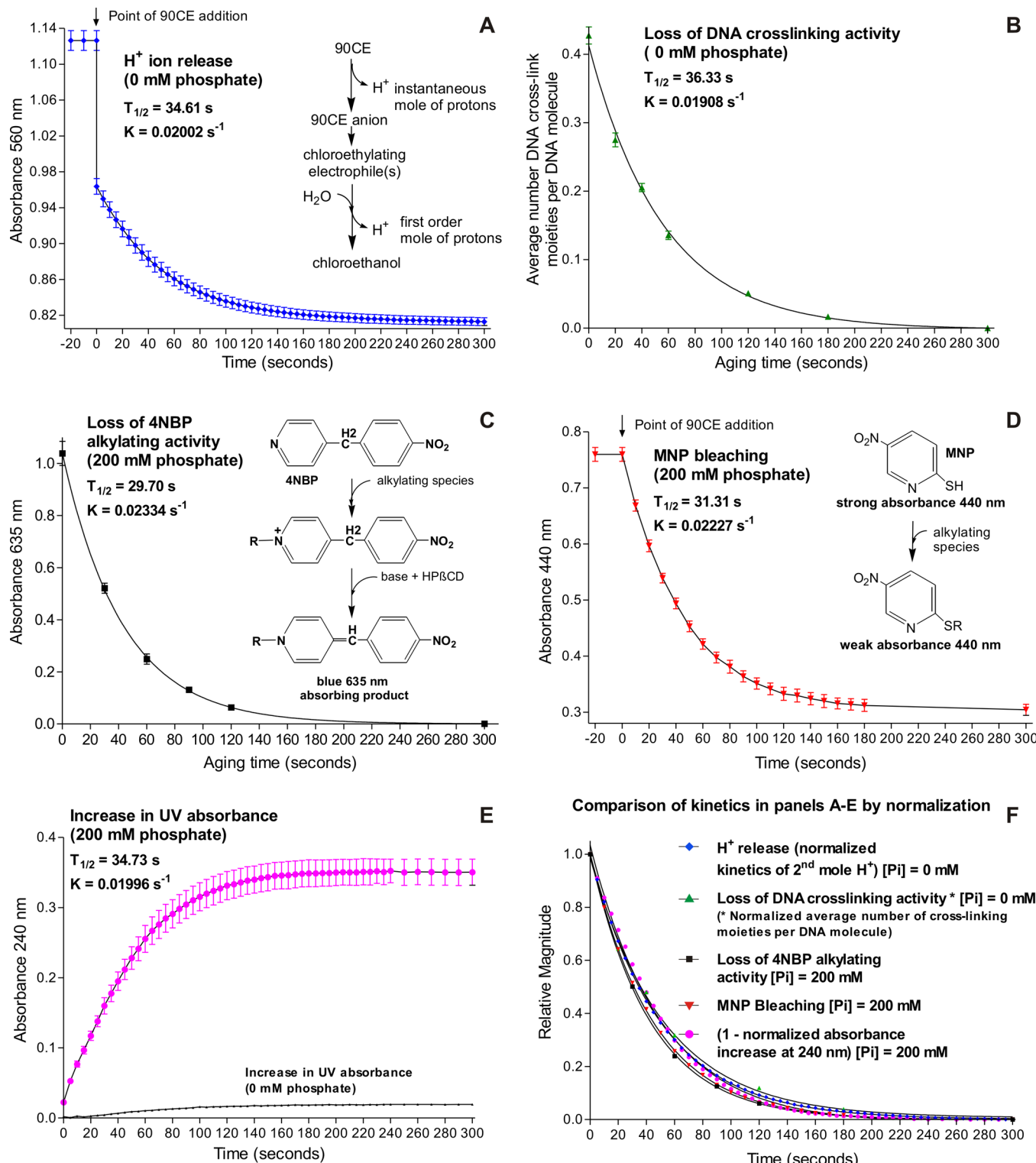


**Figure 6.** Kinetics of various 90CE dependent processes at 37 °C and pH 7.4 under high and low Pi conditions. (Panel A) Hydrogen ion generation versus time (0 mM Pi); (panel B) loss of DNA cross-linking activity versus time (0 mM Pi); (panel C) loss of 4NBP alkylating activity versus time (200 mM Pi); (panel D) MNP bleaching versus time (200 mM Pi); (panel E) generation of UV absorbing material (240 nm) versus time in the presence (upper trace) and absence (lower trace) of 200 mM Pi; and (panel F) comparison of the kinetics of the processes in panels A–E by normalization. The calculated  $t_{1/2}$  and first order rate constant, determined by a nonlinear regression best curve fit analysis, for each reaction is given in the corresponding panel. All values are the result of at least 3 determinations  $\pm$  SE.

Pi) and to alkylate 4NBP (200 mM Pi) upon aging (Figure 6, panels A–E). Essentially identical half-reaction times of approximately 35, 31, 33, 36, and 30 s, respectively, were determined for all of these processes. The generation of UV

absorbing product(s) (16-fold greater under high Pi conditions) occurs with the inverse kinetics of the other processes (exponential association rather than decay). The kinetics of all of these exponential decay processes and the exponential

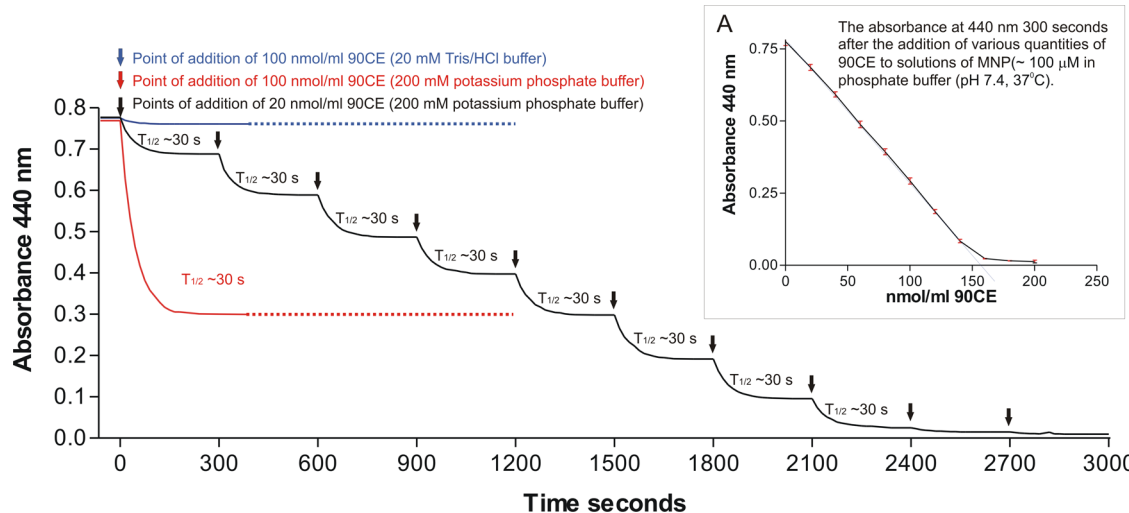


**Figure 7.** Stoichiometry of MNP ( $\sim 100 \mu\text{M}$ ) absorbance bleaching at 440 nm by 90CE at  $37^\circ\text{C}$  and pH 7.4 in 200 mM Pi and 20 mM Tris-HCl buffers. Blue trace, bleaching of MNP ( $\sim 100 \mu\text{M}$ ) by 100  $\mu\text{M}$  90CE in 20 mM Tris-HCl buffer; red trace, bleaching of MNP ( $\sim 100 \mu\text{M}$ ) by 100  $\mu\text{M}$  90CE in 200 mM Pi buffer; and black trace, bleaching of MNP ( $\sim 100 \mu\text{M}$ ) by successive 20  $\mu\text{M}$  additions of 90CE until MNP exhaustion in 200 mM Pi buffer. (Insert A) Plot of the absorbance of a MNP ( $\sim 100 \mu\text{M}$ ) solution at 440 nm, 300 s after the addition of various quantities (0–200  $\mu\text{M}$ ) of 90CE at  $37^\circ\text{C}$  and pH 7.4 in 200 mM Pi, indicating the stoichiometry of MNP titration. All values are the result of at least 3 determinations  $\pm$  SE.

association process are compared by normalization in Figure 6, panel F (1 minus the normalized value has been plotted in the case of the exponential association). Thus, the same rate determining step, i.e., the previously identified elimination of the methanesulfinate from N-1, appears to control all of these processes. Two of these processes, the kinetics of hydrogen ion generation at 0 mM Pi and the kinetics of the production of UV absorbing material at 200 mM Pi, were also examined at  $20^\circ\text{C}$  where the kinetics of both processes were equivalently slowed by a factor of  $\sim 7$ -fold (data not shown). These findings indicate that the rate determining steps for these two processes (one at 0 mM Pi and the other at 200 mM Pi) have both the same values and temperature dependencies, further implying the equivalency of their rate determining steps. Because of inherent assay physical limitations, measurements of the kinetics of hydrogen ion generation are restricted to weakly buffered solutions. Therefore, equivalent experiments could not be performed under high Pi concentrations; however, hydrogen ion liberation assays would be blind to a switch from methanesulfinate to chloride liberation since both would be accompanied by the liberation of a single hydrogen ion. The increase in the production of UV absorbing species under conditions of high Pi concentration could imply the acquisition of double bonds, and this finding would be consistent with the elimination of HCl from the chloroethyl moiety. This would be favored after the elimination of the N-1 methanesulfinate moiety because it would then result in extended conjugation from the alkyl moiety all the way to the oxygen atoms on the remaining sulfonyl moiety. This would generate  $\text{CH}_3\text{SO}_2\text{N}=\text{NCH}=\text{CH}_2$ , a very thiophilic Michael type acceptor, which would retain one of the methanesulfonyl moieties and the nitrogen atoms upon reaction with a thiol.

The loss of activity upon aging of 90CE for DNA cross-link formation (0 mM Pi) (Figure 6, panel B) and 4NBP alkylation (200 mM Pi) (Figure 6, panel C) indicate that neither the oxophilic nor thiophilic alkylating species persists in these reaction mixtures since the residual activity matches the kinetics for the rate determining elimination of the N-1 methanesul-

nate moiety and thus is only equal to the remaining 90CE in both cases. Therefore, the half-lives of both the oxophilic and thiophilic alkylating species must be considerably less than the 30 s rate determining elimination step at  $37^\circ\text{C}$  and pH 7.4.

The bleaching upon alkylation of highly chromophoric MNP at 440 nm is particularly useful since this can be used to follow real time alkylation by the thiophilic alkylating species as no workup is required. Therefore, some additional studies were performed in which MNP (100 nmol/mL) was progressively titrated by the repeated addition of initially limiting quantities of 90CE (20 nmol/mL) until the MNP was completely exhausted (Figure 7). During these successive additions, the same half-reaction time ( $\sim 30$  s) and extent of the reaction (20 nmol 90CE bleached  $\sim 12.6$  nmol of MNP) was observed until the MNP was nearly completely consumed, despite the fact that initially there was a 5-fold molar ratio of MNP to 90CE, and when the sixth aliquot was added, this was reduced to only 1.2-fold. In the presence of 200 mM Pi,  $\sim 83\%$  of the 90CE reacts via the chloride liberating pathways, which would largely comprise the Pi catalyzed thiophilic electrophile pathway and the potential minor pathway A, while the remaining  $\sim 17\%$  results in chloroethanol formation. Thus,  $\sim 14$ – $16$  nmol of the 20 nmol of 90CE would be expected to decompose via the phosphate catalyzed chloride liberating pathway, and 12.6 nmol (80–90%) of this was trapped by reacting with MNP. Since this trapped fraction appeared to be independent of the MNP concentration until exhaustion, implying extremely fast and efficient scavenging (Figure 7, panel A), it is possible that this small discrepancy reflects the presence of another minor reaction pathway that occurs in the presence of Pi (potential minor pathway B) and not merely a failure of the MNP to fully scavenge the short-lived thiophilic electrophile generated.

*In situ* generated MNP was chosen as a reagent to trap and identify the soft thiophilic electrophile because it efficiently scavenged the thiophilic species but would be expected to feebly trap any hard oxophilic electrophiles, resulting in few trapped products. Furthermore, the strong UV absorbance at 340 nm of the nitropyridine moiety is largely independent of

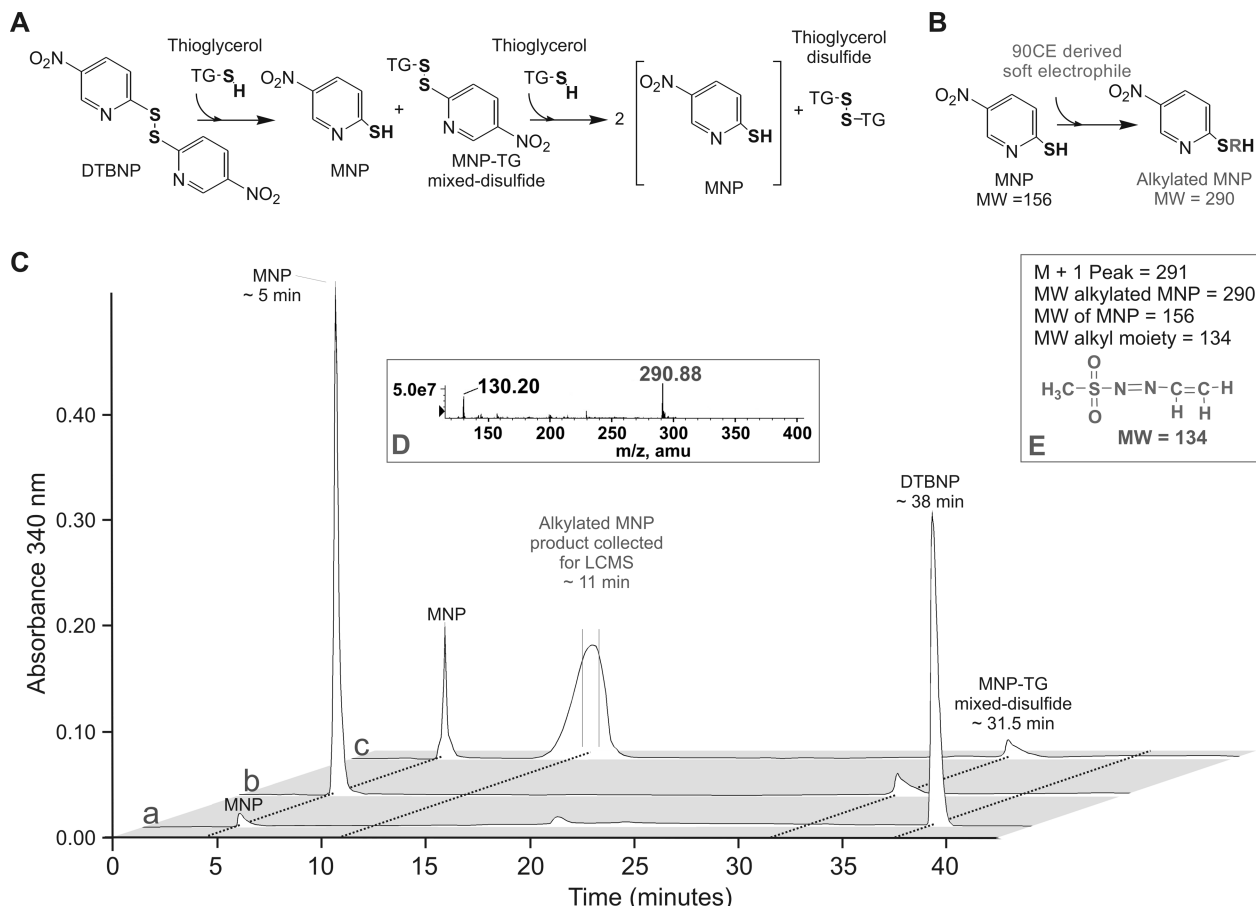


**Figure 8.** Trapping of the 90CE derived thiophilic electrophile using *in situ* generated MNP. (Panel A) Scheme illustrating the two stage reduction by TG of DTBPNP to yield 2 mol of MNP. (Panel B) Scheme illustrating the trapping of the thiophilic electrophile derived from 90CE. (Panel C) HPLC traces recorded at 340 nm of 10-fold dilutions of reactions conducted in 200 mM Pi buffer. Trace (a), 100  $\mu$ M DTBPNP (prereduction); trace (b), DTBPNP postreduction by two molar equivalents of TG to yield MNP  $\sim$  200  $\mu$ M; trace (c), postreaction of *in situ* generated MNP with a molar equivalent of 90CE indicating the production of a trapped product eluting at  $\sim$  11 min. (Insert D) LCMS analysis of the trapped product (eluting at  $\sim$  11 min), indicating a molecular plus hydrogen cation combined mass of  $\sim$  291 ( $[\text{M} + \text{H}]^+$   $\sim$  291). (Insert E) Calculation of the molecular weight of the donated alkyl moiety and postulated entity.

the state of reduction, oxidation, or alkylation of the thiol group, aiding the detection of any MNP derivatives formed. Moreover, since we suspected that the thiophilic electrophile was a Michael type acceptor, produced by the loss of HCl from the primary chloroethylating species, the resultant MNP adduct would be expected to be a neutral species suitable for LCMS. Schemes illustrating the *in situ* reduction of DTBPNP by TG to yield 2 mol of MNP and its subsequent reaction with 90CE derived electrophiles in the presence of 200 mM Pi are shown in Figure 8, panels A and B. HPLC analysis of DTBPNP gave a large 38 min peak for the oxidized material (Figure 8, panel C and trace a), and reduction by a stoichiometric quantity of TG largely converted the DTBPNP to MNP eluting at  $\sim$  5 min and a trace of the mixed disulfide eluting at  $\sim$  31.5 min (Figure 8, panel C and trace b). Treatment of this reduced material with 90CE in the presence of 200 mM Pi resulted in an 80% decrease in the area of the 5 min MNP peak and the appearance of a single new broad tailing peak (10–13 min, peak 11.6 min) for the trapped product (Figure 9, panel C and trace c). LCMS analysis of collected material eluting between 11 and 12 min indicated a mass of  $\sim$  291 for the M+1 peak of the trapped MNP derivative (Figure 8, insert D), which corresponded to a mass increase due to the electrophile moiety of 134 (Figure 8, insert E). For a Michael type acceptor, this

would equal the mass of the attacking electrophile. This mass corresponds to the mass of our proposed thiophilic electrophile  $\text{CH}_3\text{SO}_2\text{N}=\text{NCH}=\text{CH}_2$ . Reaction of this electrophile with a thiol adds the following moiety  $\text{CH}_3\text{SO}_2\text{NHN}=\text{CHCH}_2^-$  to the sulfur atom. Such adducts to both glutathione and *N*-acetylcysteine were previously postulated based on MS/NMR studies of the electrophilic metabolites of isotopically labeled laromustine and 90CE conducted at a Pi concentration of 100 mM.<sup>34</sup> It should be noted that the use of thiol traps would not be useful in trapping and identifying oxophilic or even thiophilic chloroethylating species because any adducts that were formed would rapidly eliminate the chloride to form a reactive cyclic sulfonium ion via an intramolecular nucleophilic substitution reaction and then react further with surrounding nucleophiles.

We examined 28 different anions/solutes including several phosphate esters to determine if other solutes behaved like Pi and increased the yields of soft electrophilic species from 90CE (Figure 9). Nonphosphate containing anions of strong acids exhibited very little activity over the small effect due to the copresence of 20 mM Tris-HCl, the addition of which was required to add buffering capacity. All reactions containing nonphosphate agents with  $pK_a$  values in the vicinity of the experimental pH (EDTA, carbonate, citrate, imidazole, MOPS,

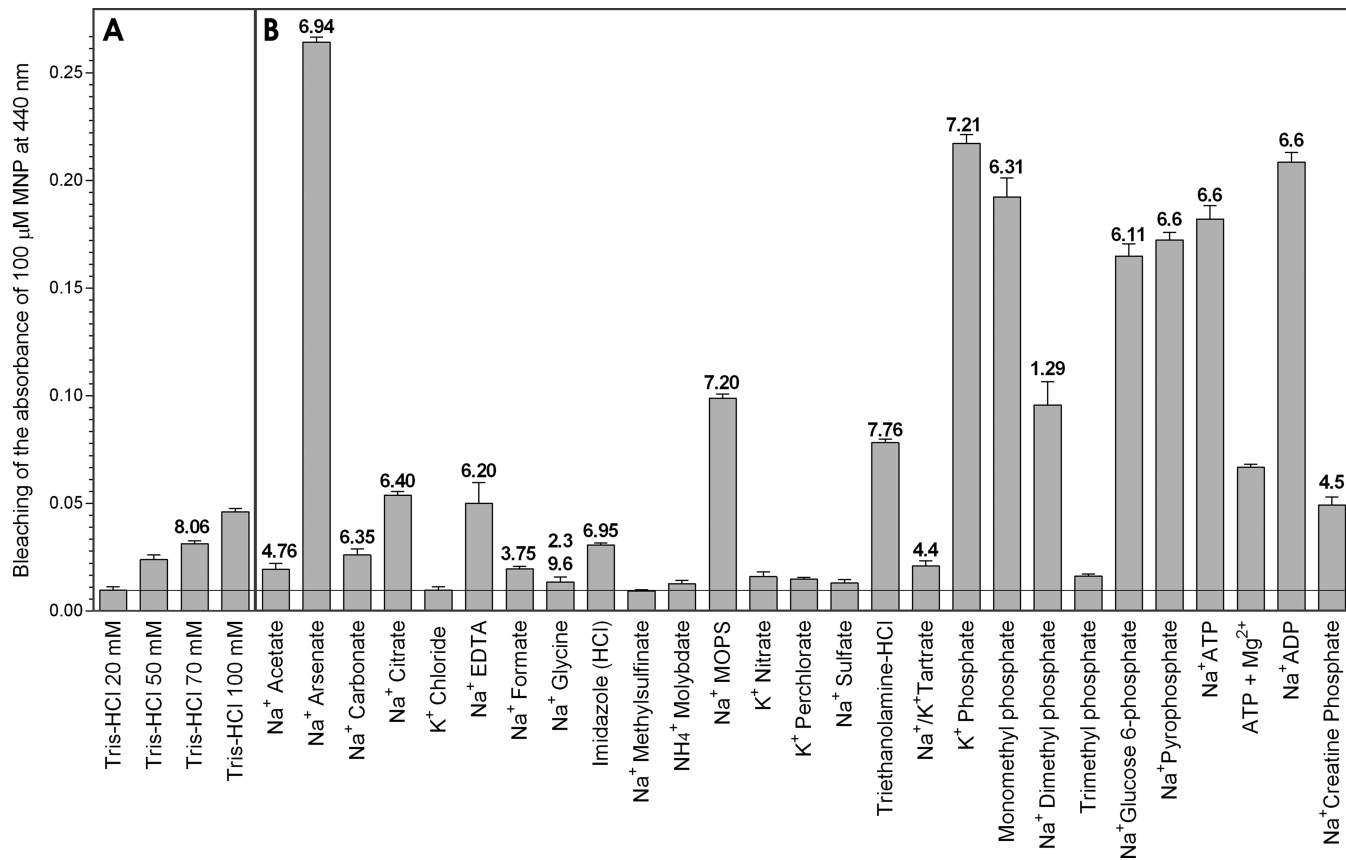


**Figure 9.** Effects of various solutes on the generation of thiophilic species from 90CE as measured by the bleaching of MNP. (Panel A) Bleaching of the absorbance of a 100  $\mu\text{M}$  MNP solution in various concentrations of Tris-HCl buffer at pH 7.4 and 37 °C at 440 nm, 300 s after the addition of 100  $\mu\text{M}$  90CE. (Panel B) The bleaching of the absorbance of a 100  $\mu\text{M}$  MNP solution in 20 mM Tris-HCl at pH 7.4 and 37 °C at 440 nm, 300 s after the addition of 100  $\mu\text{M}$  90CE supplemented with various solutes at 50 mM (adjusted to pH 7.4). The horizontal line above the x-axis represents the magnitude of MNP bleaching due to the presence of 20 mM Tris-HCl at pH 7.4 in these solute solutions (the addition of 20 mM Tris-HCl was required as many of these solutes lack buffering capacity at pH 7.4). The numerical values above the bars are the  $\text{pK}_a$  values of the added components.<sup>35–38</sup> The Mg<sup>2+</sup> ATP sample contained 52.5 mM MgCl<sub>2</sub> in addition to 50 mM ATP. The monomethylphosphate sample was as its bis(cyclohexylammonium) salt. All values are the result of at least 3 determinations  $\pm$  SE.

triethanolamine-HCl, and Tris-HCl with  $\text{pK}_a$  values of 6.20, 6.35, 6.40, 6.95, 7.20, 7.76, and 8.06, respectively)<sup>35,36</sup> contain relatively high concentrations of potentially catalytic Brønsted-Lowry bases, and these all exhibited at least some to moderate activity. Therefore, the mechanism by which these components catalyze the elimination of hydrogen chloride from the primary chloroethylating species probably involves a general acid/base catalyzed elimination reaction. However, factors other than the  $\text{pK}_a$  value appear to influence the catalytic efficiency since phosphoesters exhibited greater activity than other agents (excluding arsenate) with comparable  $\text{pK}_a$  values. We examined the activity of the three methyl esters of phosphate (monomethylphosphate, dimethylphosphate, and trimethylphosphate) since these successively replace the acidic protons of triprotic phosphoric acid and have relatively little steric bulk compared to other possible esters. Compared to Pi ( $\text{pK}_a$  7.21),<sup>37</sup> monomethylphosphate ( $\text{pK}_a$  6.31)<sup>38</sup> was found to be approximately equiactive, while dimethylphosphate ( $\text{pK}_a$  1.29)<sup>38</sup> surprisingly retained half the activity of Pi despite being a relatively strong acid, and trimethylphosphate was inactive. This finding implies that at least one of the protic sites on Pi must be unblocked for catalytic activity. Glucose 6-phosphate ( $\text{pK}_a$  6.11),<sup>38</sup> a slightly more sterically hindered and acidic phosphomonoester, was only a little less active than monomethylphosphate. A number of polyphosphates were also

examined (ATP, ADP, and pyrophosphate), and these all proved to be approximately equiactive with Pi; thus, the addition of successive phosphate groups in a linear conformation does not significantly increase activity (Figure 9). Most (~80%) of the intracellular ATP pool exists as a Mg<sup>2+</sup> chelate, owing to the strong binding affinity of ATP for Mg<sup>2+</sup>.<sup>39</sup> Since this chelation involves the two terminal phosphates,<sup>40</sup> we suspected that it may impact ATP's ability to facilitate a switch in the decomposition pathway. Therefore, the activity of ATP-Mg<sup>2+</sup> was assessed using a slight molar excess of MgCl<sub>2</sub>; this resulted in a 60% reduction in activity over that of ATP alone. Phosphocreatine (creatine phosphate) ( $\text{pK}_a$  4.5),<sup>38</sup> a guanidino phosphate in which a relatively acidic phosphate is involved in a N-phosphoguanidine linkage and a hydrogen bond with the guanidine moiety at physiological pH values, had 1/4th the activity of Pi (Figure 9). The only tested anion found to be superior to Pi was arsenate, which can be viewed as a Pi analogue. Arsenic, like phosphorus, is a group 15 element and has very similar chemical properties; moreover, arsenic acid (H<sub>3</sub>AsO<sub>4</sub>) and phosphoric acid (H<sub>3</sub>PO<sub>4</sub>) have analogous structures and near identical  $\text{pK}_a$  values of ( $\text{pK}_{a1} = 2.19$ ,  $\text{pK}_{a2} = 6.94$ , and  $\text{pK}_{a3} = 11.5$ ) and ( $\text{pK}_{a1} = 2.12$ ,  $\text{pK}_{a2} = 7.21$ , and  $\text{pK}_{a3} = 12.67$ ) for arsenic and phosphoric acids, respectively.<sup>37</sup>

The decomposition pathways open to 90CE are summarized in Figure 10. Two major decomposition pathways dominate,

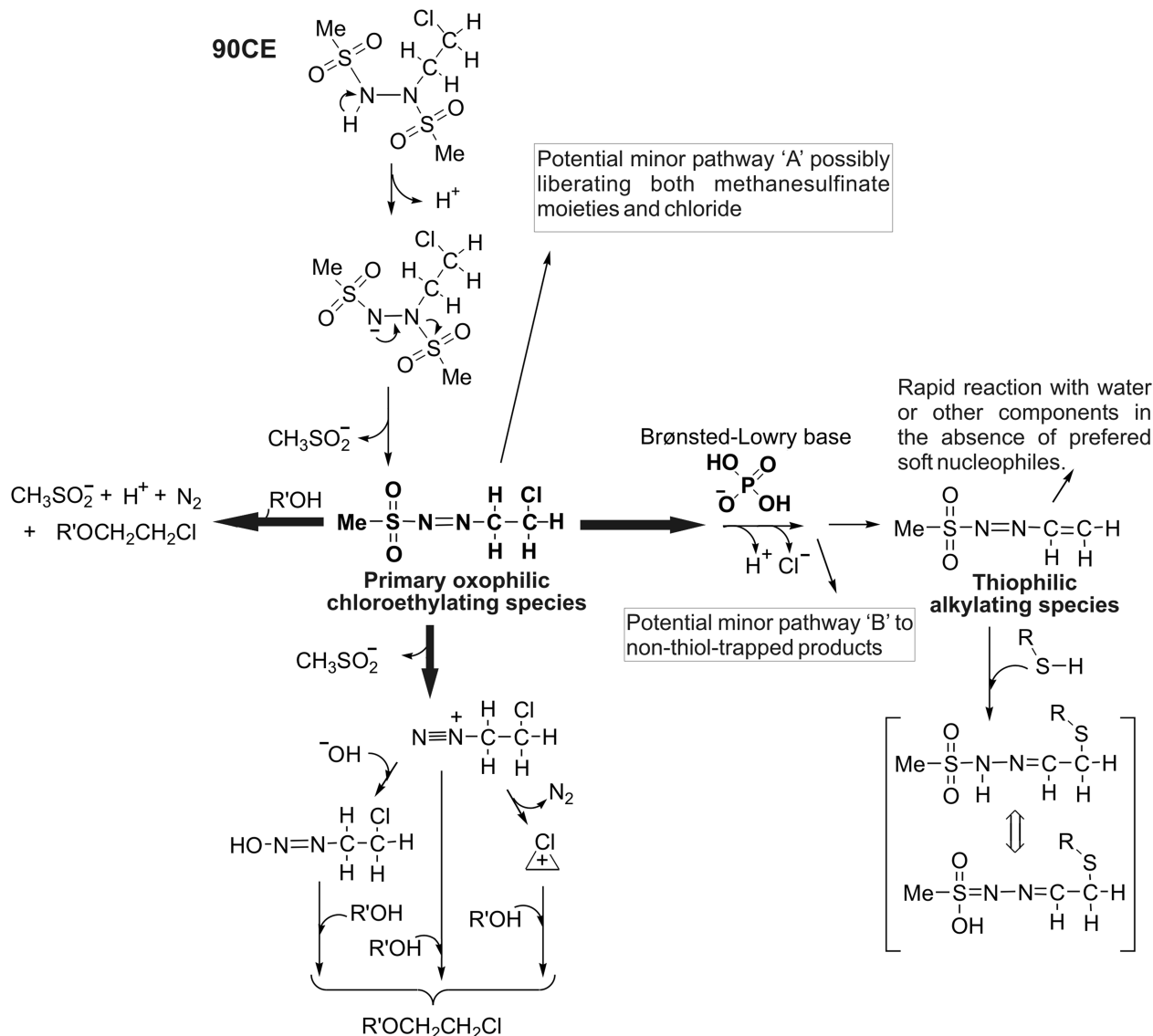


**Figure 10.** Scheme illustrating the proposed decomposition pathways for 90CE in the presence and absence of Pi or catalytic Brønsted-Lowry base. The aqueous decomposition of 90CE ( $\text{pK}_a \sim 6.5$ ) begins with the rate determining elimination of methanesulfinate ( $t_{1/2} \sim 30$  s) from the 90CE anion to generate the primary oxophilic chloroethylating species. This intermediate can chloroethylate oxygen based nucleophiles ( $\text{R}'\text{OH}$ ) directly or via the potential generation of secondary oxophilic chloroethylating species resulting in the liberation of a further mole of protons and methanesulfinate and a mole of nitrogen. In the presence of Pi or suitable Brønsted-Lowry base,  $\text{HCl}$  is eliminated, generating a short-lived highly thiophilic conjugated soft electrophile which retains the remaining methylsulfonyl moiety and both nitrogens on reaction with a thiol based nucleophile ( $\text{R}'\text{SH}$ ). The positions of two potential minor pathways (A and B) are also indicated that could account for the generation of small yields of acetaldehyde/ethylene glycol and minor discrepancies in the anticipated yields of some of the major products.

one resulting in the generation of the therapeutically important hard oxophilic chloroethylating species, which accounts for >80% of the flux in Tris-HCl buffers. The second pathway is facilitated by the presence of Pi and some phosphoesters and generates a novel soft thiophilic electrophile ( $\text{CH}_3\text{SO}_2\text{N}=\text{NCH}=\text{CH}_2$ ), which is currently thought to have little therapeutic relevance. This pathway contributes ~80% of the flux at Pi concentrations of 200 mM or greater. A number of minor pathways undoubtedly occur (potential minor pathways A and B, Figure 10) as evidenced by the generation of small yields of acetaldehyde/ethylene glycol and minor discrepancies in the anticipated yields of some of the major products. Some of these discrepancies could be explained if the pathways that generated acetaldehyde/ethylene glycol resulted in the liberation of both sulfinate moieties in addition to chloride.

The generation of highly cytotoxic G-C ethane DNA interstrand cross-links arising from DNA guanine O-6 chloroethylation, caused by the oxophilic chloroethylating species, is critical to the antineoplastic activity of 90CE. These guanine O-6 lesions are specifically repaired by MGMT, and a 22-fold greater clonogenic LC<sub>90</sub> value was observed in L1210 cell lines expressing MGMT.<sup>15</sup> This result implies that the total cytotoxicity due to the alkylation of all other biomolecules by both the oxophilic and thiophilic alkylating species, in these MGMT deficient cells, is probably ~5% of that due to guanine O-6 chloroethylation. Thus, the thiophilic electrophiles probably contribute little to the overall cytotoxicity. Moreover, it is expected that the vast majority of the thiophilic electrophiles would be scavenged by glutathione. In the presence of normal intracellular Pi and phosphate ester

concentrations, it is likely that 10–25% of the 90CE reacts via the thiophilic pathway, and this can be regarded as a loss of potentially active agent. Therefore, increases in the concentration of intracellular Pi and active phosphoesters could contribute to the total tumor resistance by decreasing the yields of the therapeutically relevant oxophilic electrophiles. Such a resistance mechanism would be expected to be limited to low level resistance (~2-fold) to 90CE prodrugs. The overall sensitivity of a tumor cell would be the product of several major and minor factors, including the DNA repair activities of MGMT and HDR, protective glutathione-S-transferases able to intercept a portion of the oxophilic electrophiles prior to reaction with DNA,<sup>41</sup> and the levels of Pi and phosphoesters able to divert the decomposition pathway away from oxophilic chloroethylating electrophile generation.

Aberrant microvascular systems in solid tumors result in hypoxic regions where the O<sub>2</sub> concentrations can approach anoxia.<sup>42</sup> Under these conditions, the levels of phosphocreatine and ATP/ATP-Mg<sup>2+</sup> fall markedly, while the levels of ADP, AMP, Pi, and phosphomonoesters exhibit a commensurate rise.<sup>43</sup> Since ATP/Mg<sup>2+</sup> and phosphocreatine have modest activity, while the total activities of their hydrolysis products are much greater, this change would be expected to result in a decrease in the percentage yield of oxophilic chloroethylating electrophiles. This action could contribute toward a modest resistance to 90CE prodrugs in hypoxic regions. Despite this, KS119, a hypoxically targeted prodrug of 90CE synthesized in our laboratory, exhibits a remarkable ~5 logs of differential cell kill in *in vitro* experiments between oxic and hypoxic environments, and selective targeting in *in vivo* models.<sup>6</sup> This high degree of hypoxic selectivity is likely the result of the efficiency of the targeting system utilized by this agent. The development of 90CE analogues which eliminate or diminish the phosphate catalyzed decomposition route would be expected to remove this weakness, increase potency, and remove potential toxicities from the thiophilic electrophiles which likely do not significantly contribute to the anticancer activity.

## CONCLUSIONS

The rate determining step in the generation of reactive electrophiles from 90CE at pH 7.4 and 37 °C involves the initial elimination of the N-1 methylsulfinate moiety ( $t_{1/2} \sim 30$  s) from the 90CE anion. After this point, two major routes of further decomposition exist: (i) generating therapeutically relevant hard oxophilic chloroethylating electrophiles and (ii) a pathway producing a soft thiophilic electrophile (CH<sub>3</sub>SO<sub>2</sub>N=NCH=CH<sub>2</sub>) currently of no known therapeutic importance (Figure 10). At this branch point, the proportion taking pathway (ii) is likely stimulated by the presence of Brønsted-Lowry bases, with Pi and its mono- and diesters appearing to be the most potent influencing molecules of biological significance. It is expected that 10–25% of 90CE decomposition proceeds via this thiophilic route under normal cellular Pi/active Pi ester concentration conditions, and this percentage is likely to increase further under hypoxic conditions. This decomposition pathway could potentially lead to novel resistance mechanisms whereby intracellular levels of Pi/active Pi esters or other catalytically active Brønsted-Lowry bases are elevated in concentration, imparting cells with modest resistance to 90CE and its prodrugs.

This study highlights the largely overlooked influence that seemingly inert reaction mixtures and/or buffer components

can potentially have on reaction pathways. While the generation of electrophiles from 90CE probably represent an extreme case, it may be prudent to conduct initial studies in a range of buffers or in buffers resembling the cellular milieu to detect such influences, or to ensure that the data obtained are physiologically relevant. We are currently designing 90CE analogues which are expected to diminish this Pi catalyzed route with the aim of increasing the yields of oxophilic chloroethylating species. These analogues are likely to be superior to 90CE when incorporated into hypoxia targeted prodrugs and would lack potential toxicities arising from the generation of thiophilic electrophiles.

## ASSOCIATED CONTENT

### S Supporting Information

A more comprehensive version of Figure 2 containing additional graphical information concerning the alkylation of 4NBP by 200 μM 90CE in the presence of 1 mM TG and by 200 μM BCNU in the presence of 20 mM TG versus Pi concentration; and a table comparing the alkylation of 4NBP by both 90CE and KS90 in 20 mM Tris-HCl and 200 mM potassium phosphate buffers at pH 7.4 in the presence and absence of 20 mM TG. This material is available free of charge via the Internet at <http://pubs.acs.org>.

## AUTHOR INFORMATION

### Corresponding Author

\*Tel: 203-785-4524. Fax 203-737-2045. E-mail: philip.penketh@yale.edu.

### Funding

This work was supported in part by U.S. Public Health Service Grants CA090671, CA122112, and CA129186 from the National Cancer Institute and a grant from the National Foundation for Cancer Research.

### Notes

Three of the authors (Philip G. Penketh, Krishnamurthy Shyam, and Alan C. Sartorelli) are listed as inventors on U.S. Patent 5637619 which includes laromustine. Laromustine has been licensed to Nanotherapeutics Inc. by Yale University. The authors declare no competing financial interest.

## ABBREVIATIONS

4NBP, 4-(4-nitrobenzyl)pyridine; 90CE, 1,2-bis-(methylsulfonyl)-1-(2-chloroethyl)hydrazine; AML, acute myelogenous leukemia; AO, *Pichia pastoris* alcohol oxidase; AUC, area under the curve; BCNU (carmustine), 1,3-bis(2-chloroethyl)-1-nitrosourea; 2,4-DNPH, 2,4-dinitrophenylhydrazine; HDR, homology directed repair; MGMT, O<sup>6</sup>-alkylguanine-DNA alkyltransferase; DTBNP, 2,2'-dithiobis(S-nitropridine); G-C ethane cross-link, 1-(N<sup>3</sup>-cytosinyl)-2-(N<sup>1</sup>-guaninyl)ethane; HP/CD, (2-hydroxypropyl)-β-cyclodextrin; KS90, 1,2-bis(methylsulfonyl)-1-methylhydrazine; Pi, phosphate (inorganic orthophosphate); TG, α-thioglycerol; MNP, 2-mercaptop-5-nitropyridine; MOPS, 3-(N-morpholino)-propanesulfonic acid

## REFERENCES

- (1) Shyam, K., Penketh, P. G., Loomis, R. H., Rose, W. C., and Sartorelli, A. C. (1996) Antitumor 2-(aminocarbonyl)-1,2-bis-(methylsulfonyl)-1-(2-chloroethyl)hydrazines. *J. Med. Chem.* 39, 796–801.
- (2) Shyam, K., Penketh, P. G., Shapiro, M., Belcourt, M. F., Loomis, R. H., Rockwell, S., and Sartorelli, A. C. (1999) Hypoxia-selective

- nitrobenzyloxycarbonyl derivatives of 1,2-bis(methylsulfonyl)-1-(2-chloroethyl)hydrazines. *J. Med. Chem.* 42, 941–946.
- (3) Liu, L., Song, L. B., Wang, Q., Lin, X. K., Belcourt, M. F., Nassar, A., Clairmont, C., King, I., and Zheng, L. M. (2005) In vivo antitumor effects of KS119W, a water-soluble hypoxia-activated alkylating agent. *Proc. Am. Assoc. Cancer Res.* 46, 325.
- (4) Pigneux, A. (2009) Laromustine, a sulfonyl hydrolyzing alkylating prodrug for cancer therapy. *Idrugs* 12, 39–53.
- (5) Penketh, P. G., Shyam, K., and Sartorelli, A. C. (1994) Studies on the mechanism of decomposition and structural factors affecting the aqueous stability of 1,2-bis(sulfonyl)-1-alkylhydrazines. *J. Med. Chem.* 37, 2912–2917.
- (6) Seow, H. A., Penketh, P. G., Shyam, K., Rockwell, S., and Sartorelli, A. C. (2005) 1,2-Bis(methylsulfonyl)-1-(2-chloroethyl)-2-[[(1-(4-nitrophenyl)ethoxy]carbonyl]hydrazine: an anticancer agent targeting hypoxic cells. *Proc. Natl. Acad. Sci. U.S.A.* 102, 9282–9287.
- (7) Penketh, P. G., Shyam, K., and Sartorelli, A. C. (2000) Comparison of DNA lesions produced by tumor-inhibitory 1,2-bis(sulfonyl)hydrazines and chloroethylnitrosoureas. *Biochem. Pharmacol.* 59, 283–291.
- (8) Gerson, S. L. (2002) Clinical relevance of MGMT in the treatment of cancer. *J. Clin. Oncol.* 20, 2388–2399.
- (9) Ishiguro, K., Zhu, Y. L., Shyam, K., Penketh, P. G., Baumann, R. P., and Sartorelli, A. C. (2010) Quantitative relationship between guanine O<sup>6</sup>-alkyl lesions produced by Onargin and tumor resistance by O<sup>6</sup>-alkylguanine-DNA alkyltransferase. *Biochem. Pharmacol.* 80, 1317–1325.
- (10) Ishiguro, K., Shyam, K., Penketh, P. G., Baumann, R. P., Sartorelli, A. C., Rutherford, T. J., and Ratner, E. S. (2013) Expression of O<sup>6</sup>-methylguanine-DNA methyltransferase examined by alkyltransfer assays, methylation-specific PCR and western blots in tumors and matched normal tissue. *J. Cancer. Ther.* 4, 919–931.
- (11) Ludlum, D. B. (1997) The chloroethylnitrosoureas: sensitivity and resistance to cancer chemotherapy at the molecular level. *Cancer Invest.* 15, 588–598.
- (12) Pegg, A. E., Dolan, M. E., and Moschel, R. C. (1995) Structure, Function, and Inhibition of O<sup>6</sup>-Alkylguanine-DNA Alkyltransferase, in *Progress in Nucleic Acid Research and Molecular Biology* (Cohn, W. E., and Moldave, K., Eds.) Vol. 51, pp167–223, Academic Press, San Diego, CA.
- (13) Penketh, P. G., Baumann, R. P., Ishiguro, K., Shyam, K., Seow, H. A., and Sartorelli, A. C. (2008) Lethality to leukemia cell lines of DNA interstrand cross-links generated by cloretazine derived alkylating species. *Leukemia Res.* 32, 1546–1553.
- (14) Rockwell, S., Liu, Y., Seow, H. A., Ishiguro, K., Baumann, R. P., Penketh, P. G., Shyam, K., Akintujoye, O. M., Glazer, P. M., and Sartorelli, A. C. (2012) Preclinical evaluation of Laromustine for use in combination with radiation therapy in the treatment of solid tumors. *Int. J. Radiat. Biol.* 88, 277–285.
- (15) Ishiguro, K., Shyam, K., Penketh, P. G., and Sartorelli, A. C. (2005) Role of O<sup>6</sup>-alkylguanine-DNA alkyltransferase in the cytotoxic activity of cloretazine. *Mol. Cancer. Ther.* 4, 1755–1763.
- (16) Finch, R. A., Shyam, K., Penketh, P. G., and Sartorelli, A. C. (2001) 1,2-Bis(methylsulfonyl)-1-(2-chloroethyl)-2-(methylamino)-carbonylhydrazine (101M): a novel sulfonylhydrazine prodrug with broad-spectrum antineoplastic activity. *Cancer Res.* 61, 3033–3038.
- (17) Johnston, T. P., and Montgomery, J. A. (1986) Relationship of structure to anticancer activity and toxicity of the nitrosoureas in animal systems. *Cancer Treat. Rep.* 70, 13–31.
- (18) Coles, B. (1985) Effects of modifying structure on electrophilic reactions with nucleophiles. *Drug Metab. Rev.* 15, 1307–1334.
- (19) Weinkam, R. J., and Lin, H. S. (1979) Reactions of 1,3-bis(2-chloroethyl)-1-nitrosourea and 1-(2-chloroethyl)-3-cyclohexyl-1-nitrosourea in aqueous solution. *J. Med. Chem.* 22, 1193–1198.
- (20) Brundrett, R. B., Cowers, J. W., Colvin, M., and Jardin, I. (1976) Chemistry of nitrosoureas. Decomposition of deuterated 1,3-bis(2-chloroethyl)-1-nitrosoureas. *J. Med. Chem.* 19, 958–964.
- (21) Weinkam, R. J., and Lin, H. S. (1982) Chloroethylnitrosourea cancer chemotherapeutic agents. *Adv. Pharm. Chemother.* 19, 1–33.
- (22) Naghipur, A., Ikonomou, M. G., Kebarle, P., and Lown, J. W. (1990) Mechanism of action of (2-haloethyl)nitrosoureas on DNA: discrimination between alternative pathways of DNA base modification by 1,3-bis(2-fluoroethyl)-1-nitrosourea by using specific deuterium labeling and identification of reaction products by HPLC/tandem mass spectrometry. *J. Am. Chem. Soc.* 112, 3178–3187.
- (23) Bodell, W. J., Bodell, A. P., and Giannini, D. D. (2007) Levels and distribution of BCNU in GBM tumors following intratumoral injection of DTI-015 (BCNU-ethanol). *Neuro-Oncology* (Durham, NC, U. S.) 9, 12–19.
- (24) Penketh, P. G., Shyam, K., and Sartorelli, A. C. (1995) Spectroscopic aqueous-phase assay for alkylating activity suitable for automation or multiwell plate application. *Anal. Biochem.* 231, 452–455.
- (25) Shyam, K., Penketh, P. G., Divo, A. A., Loomis, R. H., Patton, C. L., and Sartorelli, A. C. (1990) Synthesis and evaluation of 1,2,2-tris(sulfonyl)hydrazines as antineoplastic and trypanocidal agents. *J. Med. Chem.* 33, 2259–2264.
- (26) Grassetti, D. R., and Murray, J. F., Jr. (1969) The use of 2,2'-dithiobis(S-nitropyridine) as a selective reagent for the detection of thiols. *J. Chromatogr.* 41, 121–123.
- (27) Penketh, P. G., Shyam, K., and Sartorelli, A. C. (1997) Fluorometric assay for the determination of DNA-DNA cross-links utilizing Hoechst 33258 at neutral pH values. *Anal. Biochem.* 252, 210–213.
- (28) Penketh, P. G., Shyam, K., Patton, C. L., and Sartorelli, A. C. (1996) Spectrophotometric assay for processes involving changes in hydrogen ion concentration in aqueous solution. *Anal. Biochem.* 238, 46–49.
- (29) Sahm, H., Schütte, H., and Kula, M. R. (1982) Alcohol oxidase from *Candida boidinii*. *Methods Enzymol.* 89, 424–428.
- (30) Couderc, R., and Baratti, J. (1980) Oxidation of methanol by the yeast *Pichia pastoris*: purification and properties of alcohol oxidase. *Agric. Biol. Chem.* 44, 2279–2289.
- (31) Jörg, G., and Bertau, M. (2004) Thiol-tolerant assay for quantitative colorimetric determination of chloride released from whole-cell biodehalogenations. *Anal. Biochem.* 328, 22–28.
- (32) Babbs, C. F., and Gale, M. J. (1987) Colorimetric assay for methanesulfonic acid in biological samples. *Anal. Biochem.* 163, 67–73.
- (33) Brundrett, R. B. (1980) Chemistry of nitrosoureas. Intermediacy of 4,5-dihydro-1,2,3-oxadiazole in 1,3-bis(2-chloroethyl)-1-nitrosourea decomposition. *J. Med. Chem.* 23, 1245–1247.
- (34) Nassar, A. E., King, I., and Du, J. (2011) Characterization of short-lived electrophilic metabolites of the anticancer agent laromustine (VNP40101M). *Chem. Res. Toxicol.* 24, 568–578.
- (35) Stoll, V. S., and Blanchard, J. S. (1990) Buffers: Principles and Practice. *Methods Enzymol.* 182, 24–38.
- (36) Dawson, R. M. C., Elliott, D. C., Elliott, W. H., and Jones, K. M. (1986) *Data for Biochemical Research*, 3rd. ed., Oxford University Press, New York.
- (37) Sur, R., and Dunemann, L. (2004) Method for the determination of five toxicologically relevant arsenic species in human urine by liquid chromatography–hydride generation atomic absorption spectrometry. *J. Chromatogr., B* 807, 169–176.
- (38) Kumler, W. D., and Eiler, J. J. (1943) The acid strength of mono and diesters of phosphoric acid, the n-alkyl esters from methyl to butyl, the esters of biological importance, and the natural guanidine phosphoric acids. *J. Am. Chem. Soc.* 65, 2355–2361.
- (39) Storer, A., and Cornish-Bowden, A. (1976) Concentration of MgATP<sup>2-</sup> and other ions in solution. Calculation of the true concentrations of species present in mixtures of associating ions. *Biochem. J.* 159, 1–5.
- (40) Sigel, H. (1992) Have adenosine 5'-triphosphate (ATP<sup>4-</sup>) and related purine-nucleotides played a role in early evolution? ATP, its own ‘enzyme’ in metal ion facilitated hydrolysis! *Inorg. Chim. Acta* 198–200, 1–11.
- (41) Coles, B. F., and Kadlubar, F. F. (2003) Detoxification of electrophilic compounds by glutathione S-transferase catalysis:

determinants of individual response to chemical carcinogens and chemotherapeutic drugs? *BioFactors* 17, 115–130.

(42) Wilson, W. R., and Hay, M. P. (2011) Targeting hypoxia in cancer therapy. *Nat. Rev. Cancer* 11, 393–410.

(43) Vaupel, P., Schaefer, C., and Okunieff, P. (1994) Intracellular acidosis in murine fibrosarcomas coincides with ATP depletion, hypoxia, and high levels of lactate and total Pi. *NMR Biomed.* 7, 128–136.